Bulletin of the Mineral Research and Exploration

http://bulletin.mta.gov.tr

Relationship of ore properties and alteration of the Büyük Kuluncak (Malatya) Nb - U - NTE - Zr - Li deposit

Okan PULAT[a*], Mustafa KARAKAŞ[b] and Mehmet Ali YASTI[b]

[a]*General Directorate of Mineral Research and Exploration, Western Black Sea Regional Directorate, Zonguldak, Türkiye*
[b]*General Directorate of Mineral Research and Exploration, Konya Regional Directorate, Konya, Türkiye*

Research Article

Keywords:
Niobium, Uranium, Rare Earth Element, Kuluncak, Malatya.

ABSTRACT

Rare Earth Elements (REE) + Niobium (Nb) + Uranium (U) + Zircon (Zr) + Lithium (Li) formations are investigated which are related with alkaline Upper Cretaceous - Lower Paleocene Kuluncak Syenitoid that settled by cutting the Kuluncak ophiolite in the north of Kuluncak (Malatya) town. The alkaline magma-related Büyük Kuluncak REE - Nb - U deposit, which is enriched with regard to rare metals (Nb, Zr, and Rb), is the first economic deposit of our country. The deposit formed related to alkaline characterized foid syenite, sodalite syenite, syenite, alkaline feldspar syenite rocks which intruded into Triassic - Lower Cretaceous limestones of the Domuzdağı Nappe. The REE and fluorites with related elements formed in magmatic rocks, the contact zone of these rocks with limestones, in pegmatitic intrusions and in fluorites formed with the effect of the contact metasomatism. The purpose of this study is to interpret ore properties and the alteration grade of the rocks which formed the deposit. The REE are enriched in argillized and highly argillized samples. However, the REE composition of fresh samples are relatively low. Therefore, the REE are enriched twice or three times due to the effects of alteration and argillization of the hydrothermal fluids in the parent rock and contact metasomatism and alterations that occur both syn- and post-emplacement of syenite.

Received Date: 15.12.2020
Accepted Date: 16.07.2021

1. Introduction

Hekimhan - Hasançelebi - Kuluncak region is located within the Anatolide - Tauride Belt and contains Cretaceous - Paleocene alkaline magmatic and volcanic rocks. Since our country contains important iron deposits in this region, the studies regarding the the geology of the region (Uçurum, 1992; Gürer, 1992, 1994; Dinçer, 2009; Çobankaya, 2011; Booth et al., 2012; Metin et al., 2013), the mine potential and mineralization (Ünlü and Stendal, 1989; Özgenç and Kibici, 1994; Yamık et al., 1995; Uçurum et al., 1996; Kuşçu and Erler, 1998; Kuru et al., 2006; Marschik et al., 2008; Pektaş, 2010; Öztürk et al., 2016; Öncel, 2018; Öztürk et al., 2019; Uras et al., 2019), the petrographic and geochemical properties of igneous, volcanic and ultrabasic rocks (Yılmaz, 1991; Gürer, 1996; Parlak et al., 2006; Özgenç and İlbeyli, 2009; Kuşçu et al., 2014, Camuzoğlu et al., 2017; Camuzoğlu and Bağcı, 2018), and geochemical and radiogenic isotopic data of Malatya - Kuluncak deposit by Çimen et al. (2020) were carried out.

In recent years, ore exploration methods have been developed to pave the way for our country's mining, and it has become a target to search for critical and

Citation Info: Pulat, O., Karakaş, M., Yastı, A. M. 2022. Relationship of ore properties and alteration of the Büyük Kuluncak (Malatya) Nb - U - NTE - Zr - Li deposit. Bulletin of the Mineral Research and Exploration 167, 127-148. https://doi.org/10.19111/bulletinofmre.973626

**Corresponding author: Okan PULAT, okan.pulat@mta.gov.tr*

strategic raw material resources that are suitable for the time we live in. The REEs are classified according to their exploration and depositional characteristics. In this study, the REE deposit, which crops out in large areas and grows deeper between Başören Darılı neighborhoods in Kuluncak district of Malatya province, was evaluated in terms of formation mechanism and geological - geochemical properties.

2. General Information of REE

The REE includes 15 elements in the periodic table with atomic numbers ranging from 57 (Lanthanium La) to 71 (Lutesium Lu) with chemically similar properties. In addition, scandium (Sc) and yttrium (Y) were added to the REE due to their similar atomic properties. Of these elements, Ce is the most abundant REE, and it is more abundant in the earth's crust than copper and lead. The average concentrations of REEs in the earth's crust vary between 150 - 220 ppm (Şen, et al., 2012). The REE mineralization is mainly associated with alkaline rocks and special igneous rocks called carbonatites (Şen, et al., 2012). Apart from this, the mineral concentrations containing REE are economically encountered in placer deposits. In addition, the REE mineralization is also encountered in residual deposits (residual deposits), pegmatites, Fe-oxide Cu - Au deposits (Olympic dam), and marine phosphates formed by the deep decomposition of igneous rocks (Şen et al., 2012).

3. Regional Geology

Kuluncak and its surroundings are located in the Anatolide - Tauride Belt of Okay and Tüysüz (1999) and the Eastern Taurus Belt of Özgül (1984). In the classification of Özgül (1971), this area is located within the Bozkır Union. The Triassic - Lower Cretaceous Andırın formation (dMa) (Metin et al., 2013) is located at the bottom of the study area. The Upper Cretaceous - Paleocene Kuluncak syenitoid (Çimen et al., 2020) (Sy and Syp) was emplaced by cutting the Andırın formation. Recent fan deposits (Qym) unconformably overlie both formations. The location map of the study area is given in Figure 1.

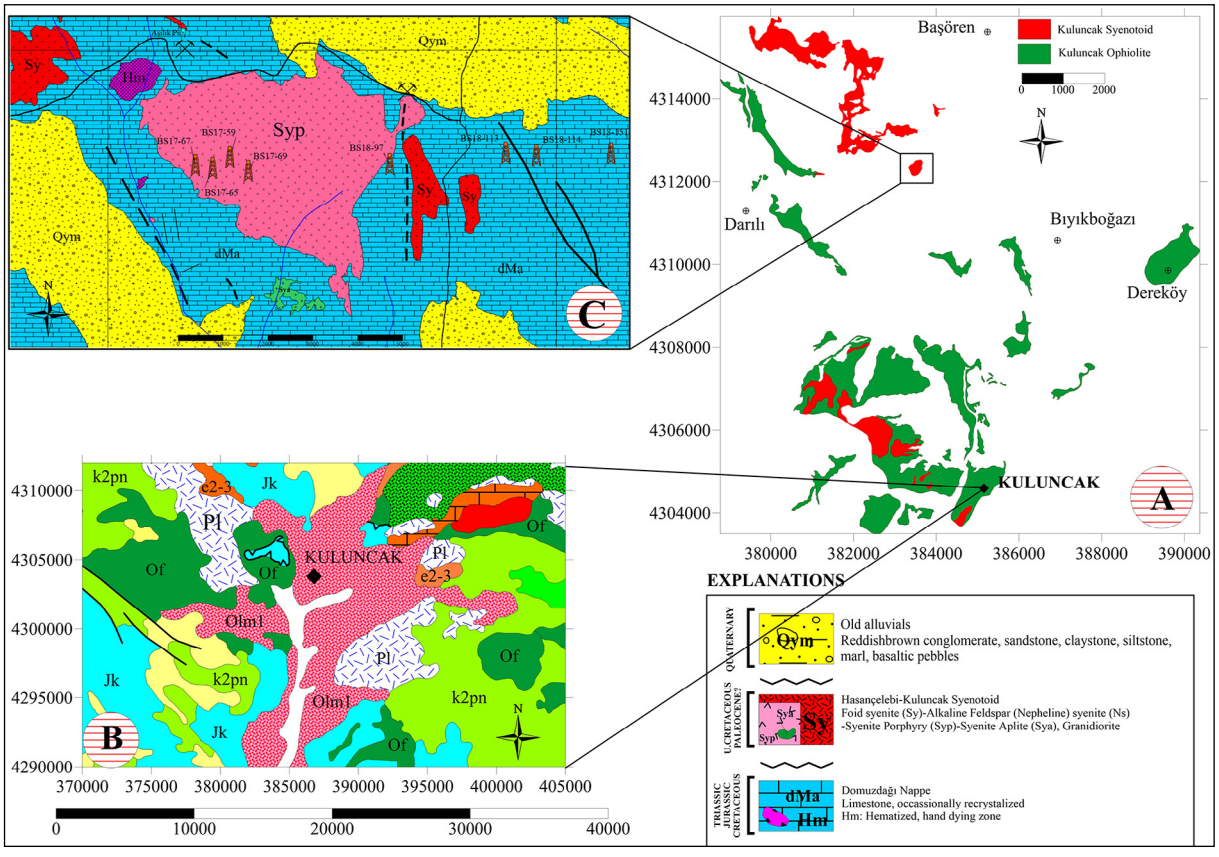

Figure 1- a) Location map of the study area within the regional ophiolitic and syenitoid masses, b) its location within the regional geology, and c) its location on the detailed geology map (Metin et al., 2013).

3.1. Andırın Formation (dMa)

The formation with thickly bedded megalodonts is partly small and accompanied by limestones with different coral species. They are laterally and vertically transitional with dolomite-dolomitic limestones. Their middle and upper levels are generally medium-thick, sometimes thinly bedded, oolitic, partly coarse miliolitic, partly dolomitic, locally chert plastered, rudist - limestone - milliolide at the top, and alternate with oolitic limestone. Especially in the middle sections, the unit consists of sparse radiolarian limestone - recrystallized limestones (Metin et al., 2013). Very coarse crystalline calcites are observed at the contacts of the limestones with the syenites cut in the drillings. Coarse calcite formations in the form of belts are observed at the contact of syenite in and around Alçakçal Hill.

3.2. Kuluncak Syenitoid (Sy)

The Kuluncak syenitoid consists of depth rocks are defined as foid syenite, syenite, quartz syenite, foid monzo syenite, foid monzo diorite, and foid monzo gabbro. They are seen in light burgundy and honey colors on their fresh surfaces. Syenitic rocks, which cover an area of 4 km^2 on their widest outcrops have equal size, medium grain, and holocrystalline texture. Medium-grained syenites in light gray and white colors in Kuluncak outcrops have an alkali feldspar syenite character. The mineralogical - petrographic properties of the rock, which is defined as foid syenite taken from the outcrops around Kuluncak, consists of alkaline feldspar, plagioclase, pyroxene crystals and pseudomorphs with holocrystalline texture (Metin et al., 2013). In petrographic studies; alkaline feldspar syenite, syenite, foid monzo syenite, foid monzo diorite, foid monzo gabbro, foidolite, feldspars, calcsilicatic rock, vesuvian garnet feldspars, nepheline foidolite, foyaite porphyry, microfoyaite, sodalite syenite, garnet type rocks were distinguished. Figure 2 shows coarse pyroxene aegirite crystals and coarse albite crystals. Intense phylogopite and vermiculite formations with garnet skarn zones were observed at the contact zones where the syenites cut carbonates. Sodalite minerals in the foid syenites are large enough to be seen with the naked eye. Figure 3 shows nepheline phenocrysts in the form of pinkish-white partially rounded, partially angular crystals in the pyroxene-rich matrix. In Figure 3, the transformation of orthoclases to albite in sodium-enriched the magma is seen.

Figure 2- Appearance of coarse pyroxene and albite crystals.


Figure 3- Foid syenite in which orthoclases are transformed to albite.

3.3. Alluvial Fan Deposits (Qym)

Alluvials consist of gravelly, sandy, clayey sedimentary deposits. Slope debris is frequently seen on the skirts of units forming steep slopes, especially the Yamadağı volcanics. The detailed geological map of the study area is given in Figure 4.

4. Material and Method

Fresh and altered core samples taken from different depths of 8 of the drillings during the resource - reserve study were used between Darılı and Başören neighborhoods in Kuluncak district of Malatya. The samples were halved from the core boxes with diamond cutters, and the halved samples were reduced to a size of less than 1 cm in a jaw crusher. The

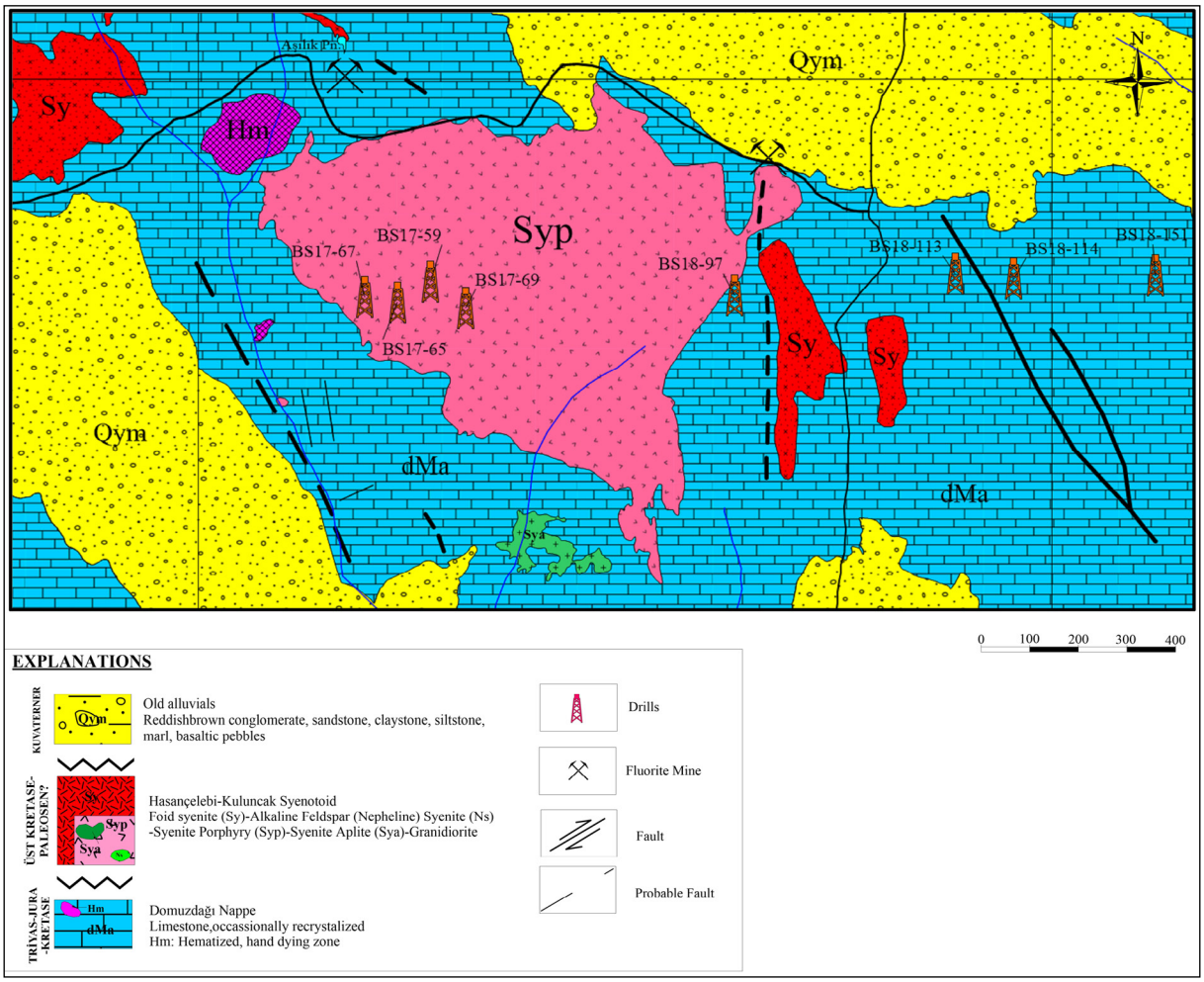

Figure 4- Location of wells and detailed geological map of the study area.

samples coming out of the jaw crusher were separated by quadrature (quartering) and sent to analysis and reserved as a witness sample. Approximately 1 kg of the sample, which was sent to analysis, was ground to powder size in a ring mill and made ready for the analysis. The samples sent to the Mineral Analysis Department of Mineral Research and Exploration of the General Directorate (MTA) were analyzed using ICP - OES (Thermo - AGILINT brand), ICP - MS (Analytical Jena), and XRF (Panalytical) devices.

5. Findings

5.1. Geochemical Analyses

The samples used in the study were taken from 8 wells drilled in the W - E direction. A total of 66 samples were taken from core samples near the surface, at middle depths, and near the bottom of the boreholes, representing the entire well.

The results of the geochemical analysis of the samples defined as fresh, altered - argillized, and highly altered - highly argillized were used in core hand samples. Fresh samples (T) are the examples that preserve the unity of the rock, hard enough to break with a hammer, and the minerals in it can be seen and identified with the naked eye. Highly altered and highly argillized samples (İB - İK) are examples in which the unity of the rock is not preserved, the minerals in the rock are so weathered that they cannot be identified in any way, and they are completely fragile. Altered - argillized samples (B - K) are the samples between fresh samples and highly altered - highly argillized (İB - İK) samples. The depths from which the samples were taken are given in the charts (Tables 1 - 8). Respectively; 3 T, 2 B-K, 3 İB - İK from well BS17-59 (Table 1), 3 T, 5 İB - İK from well BS17 - 65 (Table 2), 2 T, 2 B - K, 4 İB - İK from well BS17 - 67 (Table 3), 3 T, 5 İB - İK from well BS17 -

Table 1- Major oxide, trace, and REE values (ppm) for fresh (F), altered - argillized (Al - Ar), highly altered - highly argillized (HAl -HAr) samples of the well 17/59.

Sample Name	17/59-36	17/59-118	17/59-248	17/59-361	17/59-390	17/59-400	17/59-540	17/59-797
Alteration	HAl -HAr	Al - Ar	F	HAl -HAr	F	F	HAl -HAr	Al - Ar
Depth	10.5 -11.5	35.7-36.5	78.7-79.5	114.8-115.7	128-129	132.3-133.20	195.7-196.4	359.8360.5
SiO_2	48.07	46.70	49.98	44.28	51.39	52.75	54.98	52.12
Al_2O_3	15.07	13.80	20.05	18.71	17.59	20.15	21.62	20.89
Fe_2O_3	18.42	2.33	10.98	3.11	10.03	8.25	9.11	6.26
Na_2O	2.23	3.19	5.59	1.21	2.64	3.14	4.05	6.64
K_2O	9.95	7.69	4.00	6.31	7.83	5.06	3.58	4.92
CaO	0.22	12.30	2.91	9.80	4.15	3.31	0.87	3.04
MgO	0.09	0.25	0.29	1.21	2.64	3.14	4.05	0.57
MnO	0.14	0.22	0.21	0.13	0.22	0.12	0.07	0.08
TiO_2	0.74	0.23	0.25	0.46	0.44	0.22	0.29	0.16
P_2O_5	0.10	0.10	0.10	0.10	0.10	0.10	0.10	0.10
A.Z	2.91	11.68	5.50	12.13	4.38	5.73	4.42	5.02
Y	77.37	419.19	63.54	47.55	71.49	7.15	145.98	0.93
La	366.42	436.71	180.27	111.13	181.29	26.09	819.91	2.39
Ce	644.35	975.46	312.88	171.95	540.04	39.66	1632.58	4.81
Pr	28.15	43.66	26.18	8.41	14.85	1.86	79.97	0.44
Nd	108.39	222.88	73.71	34.18	67.10	8.25	244.79	1.12
Sm	21.19	56.04	12.13	7.32	13.62	1.65	44.02	0.17
Eu	4.09	10.51	2.25	1.66	2.64	0.36	7.03	0.10
Gd	47.13	98.88	14.35	17.78	29.66	3.47	97.89	0.18
Tb	2.22	6.66	1.77	1.02	1.55	0.14	8.16	0.10
Dy	15.93	61.27	12.14	9.44	14.27	1.38	30.35	0.17
Ho	2.26	9.19	2.15	1.51	1.99	0.18	6.89	0.10
Er	11.93	52.79	7.00	9.34	12.42	1.26	16.26	0.15
Tm	0.95	4.43	0.74	0.99	1.01	0.10	1.44	0.10
Yb	7.82	45.68	4.19	10.30	11.59	1.46	6.90	0.29
Lu	0.50	2.70	0.35	0.70	0.74	0.10	0.77	0.10
Sc	0.10	0.59	0.10	0.53	0.19	0.10	0.10	0.10
ΣREEO	1338.81	2446.62	713.72	433.82	964.44	93.21	3143.02	11.25
Th	68.11	3397.37	62.39	2995.85	1479.00	16.62	130.85	1.21
U	250.72	79.24	12.26	255.18	43.98	32.65	13.77	26.84
Ta	35.05	70.06	6.95	15.82	10.42	4.99	18.96	6.24
Zr	156.26	1775.82	407.29	1368.43	1337.67	260.96	673.95	139.71
Cs	2.66	2.60	3.96	3.68	3.57	3.35	4.28	3.89
Hf	3.05	16.12	6.55	12.83	11.34	4.37	8.86	1.93
Nb	1899.22	2307.35	170.33	608.57	510.37	122.17	452.67	126.36
Rb	556.30	466.98	391.51	639.83	766.78	554.59	670.19	242.21
Be	21.34	20.64	7.44	3.57	5.22	5.55	4.58	1.11
Ge	2.43	3.42	1.52	0.90	1.71	0.80	3.17	0.73
Ga	72.48	58.66	48.47	53.73	54.72	52.91	63.97	28.59
As	117.56	88.11	40.21	57.20	20.98	14.57	63.33	11.34
Ni	5.34	3.44	0.95	17.06	1.18	1.74	7.80	0.42
Co	0.59	2.44	0.15	2.13	0.33	0.31	0.30	0.21
Li	126.35	1233	194.13	77.25	142.73	137.20	290.51	41.75
Bi	16.51	1.06	0.83	1.83	0.46	0.43	0.44	1.79
Cr	34.31	10.75	26.83	5.32	6.90	18.81	12.23	5.73
V	30.55	23.22	23.87	16.76	16.59	16.08	12.60	17.54
W	10.00	10.00	10.00	10.00	10.00	10.00	10.00	10.00
Sr	44.28	254.28	38.15	38.55	68.96	47.02	36.23	43.08
Ba	3110.23	1283.13	180.78	1047.49	1430.84	688.13	116.06	18.16
Sn	21.11	22.31	21.07	37.85	31.18	18.69	28.14	11.31
Cd	2.49	0.70	0.55	0.72	0.63	0.12	0.25	0.26
Cu	31.35	2.56	3.12	21.97	5.54	3.06	5.63	5.49
Pb	1605.49	12.11	152.57	39.72	22.23	20.50	100.59	28.01
Zn	5248.82	382.17	199.02	183.98	167.43	82.51	203.61	47.25
Mo	10.13	5.81	1.61	3.34	1.92	2.14	3.79	0.57
Sb	19.88	20.15	2.51	8.54	4.48	2.93	5.40	0.38
ΣLREE	1245.87	1678.71	593.03	325.68	803.29	75.86	2777.24	8.93
ΣHREE	92.83	114.79	14.42	22.84	27.74	3.11	32.26	92.83
Eu/Eu*	15.50	0.43	0.52	0.45	0.40	0.46	0.33	1.75
$(La/Yb)_N$	0.40	6.45	29.01	7.28	10.55	12.03	80.09	5.52
$(La/Sm)_N$	31.60	4.90	9.35	9.54	8.37	9.93	11.72	8.64
$(Ce/Yb)_N$	10.88	5.52	19.32	4.32	120.5	7.02	61.18	4.26
$(Ce/Sm)_N$	21.32	4.20	6.23	5.67	9.57	5.79	8.95	6.67
$(Eu/Yb)_N$	7.34	0.65	1.53	0.46	0.65	0.69	2.90	0.97

* REE's are normalized according to Boynton (1984).

Table 2- Major oxide, trace and REE values (ppm) for fresh (F), highly altered - highly argillized (HAl - HAr) samples of the well 17/65.

Sample Name	17/65 -4	17/65 -212	17/65 -316	17/65 -590	17/65 -725	17/65 -768	17/65 -934	17/65 -1009
Alteration	HAl - HAr	T	HAl - HAr	HAl - HAr	T	HAl - HAr	HAl - HAr	T
Depth	2 - 3	73.4-74.00	105.5-105.9	311.5-312	383 -383.8	400 -401	499.2 -500.2	542 -543
SiO_2	60.75	50.81	55.52	56.20	53.30	55.40	45.47	46.94
Al_2O_3	19.13	18.71	17.51	17.00	19.90	16.90	23.21	23.09
Fe_2O_3	5.09	5.91	8.37	5.79	5.22	5.07	4.13	5.44
Na,O	4.18	8.28	5.21	2.22	2.36	2.32	1.64	4.63
K_2O	6.92	1.51	4.44	4.37	5.43	5.62	5.84	6.31
CaO	0.47	3.08	2.99	5.38	4.75	6.35	6.06	6.64
MgO	0.17	0.78	0.40	1.25	0.54	0.60	0.99	0.61
MnO	0.18	0.09	0.16	0.10	0.18	0.08	0.10	0.21
TiO_2	0.29	0.19	0.41	0.23	0.31	0.11	0.18	0.28
P_2O_5	0.10	0.10	0.10	0.10	0.10	0.10	0.10	0.05
A.Z	2.11	9.00	4.02	6.88	7.67	7.44	12.22	5.18
Y	74.46	16.56	257.44	88.97	19.00	5.76	40.49	33.26
La	201.81	16.62	584.73	213.58	28.67	9.48	85.76	73.12
Ce	307.74	27.67	804.01	319.79	49.18	13.97	163.38	132.26
Pr	24.93	2.56	66.57	28.55	4.48	1.04	17.88	12.97
Nd	70.82	7.06	153.75	69.40	11.35	7.37	46.24	34.40
Sm	13.61	1.29	22.54	11.48	1.93	1.36	8.55	6.44
Eu	2.77	0.28	4.57	2.06	0.40	0.33	1.81	1.96
Gd	16.38	1.77	35.77	15.24	2.23	1.51	8.89	6.34
Tb	2.11	0.27	5.77	2.18	0.40	0.10	1.44	0.94
Dy	13.05	1.89	45.39	13.11	2.62	1.61	7.43	5.55
Ho	2.66	0.46	11.76	3.36	0.67	0.12	1.69	1.21
Er	8.18	1.67	44.41	10.14	2.15	1.13	4.37	3.93
Tm	0.99	0.28	7.34	1.63	0.29	0.10	0.62	0.56
Yb	5.02	1.93	44.78	8.46	2.49	1.28	2.95	3.61
Lu	0.48	0.25	4.64	1.00	0.16	0.10	0.36	0.47
Sc	0.14	0.23	1.46	0.71	0.59	0.46	0.10	0.10
ΣREEO	745.13	80.77	2094.93	789.66	126.60	45.71	391.95	317.12
Th	729.14	11.05	29.69	158.85	11.87	3.92	25.26	27.12
U	45.15	18.77	109.40	26.12	30.16	5.98	6.08	10.56
Ta	24.14	7.56	112.86	52.93	6.27	6.20	10.06	5.46
Zr	394.90	648.14	2850.21	1482.62	1266.06	340.08	226.58	183.81
Cs	4.61	161.84	4.63	23.90	8.25	5.73	23.82	322.44
Hf	5.27	8.78	38.86	17.90	7.50	6.99	3.56	3.19
Nb	502.33	142.16	1046.91	1044.02	242.30	103.74	145.78	72.16
Rb	385.22	242.99	442.68	456.03	941.58	1069.25	296.38	290.97
Be	18.59	13.35	7.32	11.83	3.55	2.53	4.66	4.48
Ge	1.05	1.08	1.33	1.48	1.51	1.28	1.11	1.24
Ga	63.13	55.53	65.49	78.56	68.02	52.37	39.69	27.14
As	67.48	30.28	34.49	113.66	23.37	23.86	36.01	17.92
Ni	2.68	0.73	6.32	85.17	3.82	6.97	31.01	15.28
Co	0.44	0.15	0.31	1.64	0.73	0.79	0.77	3.98
Li	345.80	84.51	108.32	61.96	145.56	98.09	114.71	182.86
Bi	2.04	1.42	1.07	1.79	3.81	2.16	1.31	0.29
Cr	15.25	21.42	34.12	10.83	22.55	8.18	13.49	28.04
V	22.41	27.18	27.17	18.20	29.97	70.28	41.14	37.19
W	10.00	10.00	10.00	10.00	10.00	10.00	10.00	10.00
Sr	61.15	70.73	53.76	60.51	67.67	28.85	117.75	676.60
Ba	1489.80	29.11	390.33	107.78	82.19	77.69	244.68	1817.81
Sn	18.21	22.58	39.87	24.42	10.00	18.77	10.00	10.00
Cd	0.97	0.94	1.06	1.11	0.27	0.53	0.24	0.36
Cu	21.47	5.31	4.05	8.78	7.77	1.73	4.33	4.90
Pb	21.93	504.43	724.12	122.66	7.92	16.09	44.40	30.15
Zn	638.99	343.68	242.92	673.90	137.33	122.94	204.67	220.05
Mo	6.02	1.28	2.44	3.83	2.18	4.07	1.54	2.55
Sb	13.26	1.26	3.38	20.70	1.60	6.23	3.16	0.86
ΣLREE	605.29	53.91	1609.06	631.33	93.67	31.86	313.26	252.75
ΣHREE	17.33	4.58	112.93	24.59	5.75	2.73	9.99	9.78
Eu/Eu*	0.57	0.58	0.49	0.48	0.58	0.70	0.64	0.94
$(La/Yb)_N$	27.11	5.81	8.80	17.03	7.78	4.98	19.62	13.64
$(La/Sm)_N$	9.33	8.13	16.32	11.70	9.33	4.39	6.31	7.14
$(Ce/Yb)_N$	15.86	3.71	4.64	9.78	5.12	2.82	14.34	9.47
$(Ce/Sm)_N$	5.46	5.20	8.61	6.72	6.14	2.48	4.61	4.96
$(Eu/Yb)_N$	1.57	0.42	0.29	0.69	0.45	0.72	1.75	1.54

* REE's are normalized according to Boynton (1984).

Table 3- Major oxide, trace and REE values (ppm) for fresh (F), altered- argillized (Al-Ar), highly altered- highly argillized (HAl - HAr) samples of the well 17/67.

Sample Name	17/67 - 6	17/67 - 21	17/67 -171	17/67-178	17/67-567	17/67-571	17/67-643	17/67-738
Alteration	HAl - HAr	Al-Ar	HAl - HAr	HAl - HAr	F	F	HAl - HAr	Al-Ar
Depth	2.50-3.10	7.70-8.20	49.0-49.50	50.90-51.4	325-326	328-329	362-362.4	419.6-420.2
SiO_2	58.78	53.73	54.60	55.27	54.89	53.20	47.75	47.54
Al_2O_3	19.64	18.47	19.88	15.19	19.13	22.54	21.85	22.53
Fe_2O_3	5.02	8.75	8.70	10.07	7.73	5.46	6.72	3.31
Na_2O	2.64	4.93	3.93	8.01	4.37	2.93	0.40	3.62
K_2O	8.55	3.57	2.60	1.94	5.12	5.26	6.94	4.46
CaO	0.22	2.86	2.50	3.61	3.27	3.20	1.57	7.36
MgO	0.11	0.57	0.72	0.45	0.34	0.54	1.11	0.65
MnO	0.12	0.27	0.25	0.27	0.09	0.07	0.28	0.11
TiO_2	0.62	0.48	0.41	0.52	0.12	0.08	0.79	0.10
P_2O_5	0.09	0.12	0.10	0.10	0.10	0.10	0.10	0.10
A.Z	2.19	4.22	4.92	3.38	4.66	6.42	9.80	10.17
Y	217.13	537.91	334.51	498.22	2.19	2.36	1512.15	56.05
La	417.11	1017.45	439.75	798.46	5.57	9.28	973.38	100.19
Ce	689.97	1467.40	616.99	1096.05	12.59	19.74	2413.58	187.33
Pr	56.85	119.06	47.86	83.40	0.70	1.00	213.31	21.31
Nd	127.95	255.20	92.80	174.81	5.35	6.76	1083.88	60.47
Sm	20.38	36.63	15.78	24.44	0.98	1.13	118.81	11.16
Eu	5.07	8.60	3.70	5.58	0.18	0.19	21.98	2.19
Gd	26.01	59.29	25.58	36.96	1.34	1.80	160.62	12.25
Tb	4.62	10.33	5.12	7.41	0.10	0.10	6.44	1.82
Dy	33.78	76.15	43.03	59.95	0.95	0.93	123.65	10.59
Ho	8.06	18.49	11.36	15.66	0.10	0.10	7.69	2.22
Er	27.84	62.68	44.41	59.66	0.73	0.67	78.41	6.30
Tm	4.14	8.86	7.05	9.07	0.10	0.10	2.86	0.81
Yb	23.09	48.09	42.04	52.65	1.07	0.75	51.30	4.02
Lu	2.26	4.55	4.14	5.09	0.10	0.10	1.35	0.43
Sc	0.88	2.41	1.26	2.03	0.10	0.10	0.85	0.10
ΣREEO	1665.13	3733.08	1738.39	2929.43	32.15	45.10	6770.27	477.24
Th	195.74	258.29	61.52	136.13	3.91	6.43	1187.60	26.20
U	266.75	127.37	126.05	90.57	2.15	1.27	35.02	5.73
Ta	115.26	92.40	104.13	121.21	1.03	0.64	20.20	3.39
Zr	2467.21	5918.16	3771.14	5469.30	382.20	216.92	5546.23	192.08
Cs	5.33	5.44	8.27	3.60	3.77	2.95	8.02	6.21
Hf	23.78	50.22	33.11	46.57	6.59	3.81	27.54	2.78
Nb	1944.95	1546.11	1571.69	2002.43	28.32	17.82	1377.05	68.66
Rb	733.41	415.95	285.04	221.15	702.39	727.88	908.60	208.49
Be	9.77	11.51	15.37	13.35	3.18	3.61	8.70	4.17
Ge	1.55	3.53	2.20	2.93	1.50	1.10	9.40	1.28
Ga	69.71	78.89	68.27	71.82	42.89	37.55	102.28	31.94
As	125.82	30.13	33.22	35.25	20.56	21.35	736.22	19.48
Ni	11.12	4.41	20.02	22.93	0.94	0.78	70.47	9.64
Co	0.20	0.17	0.92	0.73	0.48	0.30	5.22	0.79
Li	135.24	238.41	130.69	202.56	88.27	137.92	138.17	146.83
Bi	2.40	0.30	1.53	0.65	0.13	0.10	1.65	0.46
Cr	24.98	20.67	9.47	13.06	13.40	6.50	14.94	15.82
V	37.75	29.52	28.67	28.59	47.83	48.33	79.15	35.30
W	10.00	11.11	10.00	14.80	10.00	10.00	10.00	10.00
Sr	106.89	62.42	56.67	50.02	62.86	71.26	114.72	164.13
Ba	2009.62	462.81	425.91	219.11	73.39	49.67	8401.48	84.23
Sn	31.48	39.82	41.58	55.13	14.36	10.00	22.95	10.00
Cd	5.51	4.05	2.18	1.85	0.54	0.28	0.89	0.26
Cu	59.37	2.44	9.54	6.79	3.14	2.05	29.85	3.00
Pb	2697.58	468.88	186.85	142.30	8.61	13.28	161.61	16.20
Zn	2688.29	1098.75	576.33	614.54	97.59	83.29	740.80	134.68
Mo	5.40	1.37	2.03	3.49	2.00	1.63	13.31	1.42
Sb	8.70	5.71	4.32	3.87	1.49	2.02	11.49	1.63
ΣLREE	1291.88	2859.10	1200.40	2152.72	24.20	36.78	4684.16	369.30
ΣHREE	65.38	142.66	109.00	142.13	2.10	1.71	141.61	13.77
Eu/Eu*	0.67	0.56	0.56	0.57	0.49	0.41	0.49	0.57
$(La/Yb)_N$	12.18	14.26	7.05	10.22	3.51	8.40	12.79	16.80
$(La/Sm)_N$	12.87	17.47	17.52	20.55	3.57	5.19	5.15	5.65
$(Ce/Yb)_N$	7.73	7.89	3.81	5.38	30.4	6.85	12.17	12.05
$(Ce/Sm)_N$	8.17	9.67	9.48	10.82	3.09	4.24	4.90	4.05
$(Eu/Yb)_N$	0.62	0.51	0.25	0.30	0.49	0.73	1.22	1.55

* REE's are normalized according to Boynton (1984).

Table 4- Major oxide, trace and REE values (ppm) for fresh (F), highly altered - highly argillized (HAl - HAr) samples of the well 17/69.

Sample Name	17/69-10	17/69-33	17/69-69	17/69-147	17/69-260	17/69-340	17/69-523	17/69-689
Alteration	HAl - HAr	F	HAl - HAr	F	F	HAl - HAr	HAl - HAr	HAl - HAr
Depth	4.60-5.15	13-14	25.9-26.45	51.4-51.7	85.4-86	107-110	200.5-200.9	330.5-330.9
SiO_2	59.16	52.26	53.89	54.36	47.18	53.47	48.30	46.44
Al_2O_3	17.46	15.38	17.78	19.70	17.46	20.39	14.90	18.25
Fe_2O_3	4.41	5.98	9.27	8.26	8.09	8.96	10.50	13.04
Na_2O	1.70	1.31	2.21	4.65	3.20	4.45	0.73	0.43
K_2O	11.84	11.71	8.14	3.38	4.59	1.02	2.52	4.86
CaO	0.36	5.83	2.49	3.81	6.86	2.57	6.83	5.52
MgO	0.19	0.10	0.33	0.20	0.89	0.95	4.17	1.40
MnO	0.11	0.21	0.14	0.13	0.06	0.08	0.10	0.06
TiO_2	0.42	0.64	0.52	0.24	0.16	0.24	0.35	0.57
P_2O_5	0.10	0.13	0.10	0.10	0.10	0.10	0.10	0.10
A.Z	1.79	4.820	3.810	5.01	7.00	6.31	10.00	8.17
Y	398.02	73.42	26.93	8.59	68.88	45.25	149.29	305.88
La	1043.52	305.84	105.86	29.65	129.23	98.58	319.46	328.53
Ce	1508.29	484.12	207.68	40.74	230.37	151.56	606.31	2288.37
Pr	108.34	36.47	16.84	3.06	18.22	12.26	45.41	98.10
Nd	253.97	94.44	46.45	8.20	51.28	33.00	120.62	265.07
Sm	38.76	16.71	8.45	1.37	8.08	5.54	21.61	54.20
Eu	7.77	3.54	1.68	0.33	1.87	1.21	4.15	10.72
Gd	51.46	18.78	8.65	1.50	10.69	7.02	28.99	53.51
Tb	8.10	2.51	1.12	0.20	1.52	0.93	3.29	9.96
Dy	74.43	19.03	7.79	1.54	11.95	6.77	20.94	55.54
Ho	15.59	3.41	1.27	0.26	2.42	1.52	4.17	13.22
Er	72.96	14.20	5.00	1.11	8.95	5.52	13.89	32.09
Tm	8.98	1.64	0.57	0.13	0.95	0.64	1.79	4.53
Yb	64.87	12.09	4.53	1.14	6.29	5.19	10.06	26.65
Lu	5.00	0.98	0.43	0.12	0.48	0.46	0.97	2.25
Sc	0.82	0.10	0.10	0.10	0.87	0.78	0.52	0.48
ΣREEO	3660.88	1087.28	443.42	98.05	552.04	376.23	1351.45	3549.07
Th	293.68	674.21	48.20	6.59	28.87	16.48	293.48	3795.35
U	177.32	66.23	52.86	5.41	21.38	19.05	30.40	33.25
Ta	126.91	36.65	32.34	5.27	9.93	9.72	30.77	9.35
Zr	4403.58	561.24	357.42	235.68	867.58	1018.51	1471.29	3110.05
Cs	3.94	3.55	2.54	5.57	2.49	3.10	80.78	23.66
Hf	52.04	8.34	7.47	4.05	8.56	11.03	12.87	15.79
Nb	1643.24	698.73	605.68	124.58	140.84	193.31	919.31	1211.50
Rb	408.57	400.00	400.72	142.76	382.41	76.98	419.46	510.85
Be	7.91	10.14	8.22	7.10	3.10	7.03	7.49	9.48
Ge	1.58	0.97	1.02	0.98	1.66	1.39	1.93	3.67
Ga	70.11	59.18	53.76	48.84	49.66	54.66	64.43	78.08
As	72.70	68.03	19.92	10.90	18.96	14.99	236.21	186.93
Ni	11.70	3.10	2.73	1.33	1.72	1.47	58.93	28.32
Co	0.28	0.30	0.18	0.28	0.49	0.26	1.09	0.63
Li	151.92	162.97	180.35	229.99	235.35	168.91	495.53	74.38
Bi	0.67	2.59	1.81	1.50	6.64	1.14	1.87	0.67
Cr	9.56	16.74	12.62	15.75	21.39	6.58	3.52	5.18
V	14.74	17.08	15.07	19.01	11.39	11.11	35.18	13.51
W	14.49	10.00	10.00	10.00	10.00	10.00	10.00	10.00
Sr	34.38	327.96	47.27	52.25	272.35	89.44	58.78	70.63
Ba	1130.27	2128.26	514.08	96.60	52.39	28.21	57.56	111.23
Sn	13.45	11.38	23.65	18.18	15.62	19.40	21.82	30.55
Cd	3.00	1.59	0.83	0.58	0.86	1.19	0.89	0.73
Cu	10.19	8.89	2.22	1.51	3.46	5.06	8.28	8.20
Pb	609.58	701.14	1265.57	212.17	61.92	331.18	411.41	72.56
Zn	912.58	746.84	475.66	218.78	129.89	181.84	731.00	295.66
Mo	4.79	9.62	1.30	1.60	1.81	0.51	4.11	3.19
Sb	10.92	8.79	6.79	2.06	0.88	1.37	7.48	4.62
ΣLREE	2914.12	920.87	376.81	81.64	429.09	295.39	1091.80	2980.06
ΣHREE	167.40	32.32	11.80	2.77	19.09	13.33	30.87	78.72
Eu/Eu*	0.53	0.61	0.6	0.71	0.62	0.59	0.51	0.61
$(La/Yb)_N$	10.84	17.06	15.77	17.49	13.86	12.81	21.41	8.31
$(La/Sm)_N$	16.93	11.51	7.88	13.63	10.07	11.18	9.3	3.81
$(Ce/Yb)_N$	6.01	10.36	11.87	9.22	9.48	7.56	15.59	22.21
$(Ce/Sm)_N$	9.39	6.99	5.93	7.19	6.89	6.6	6.77	10.19
$(Eu/Yb)_N$	0.34	0.83	1.05	0.83	0.85	0.66	1.17	1.14

* REE's are normalized according to Boynton (1984).

Table 5- Major oxide, trace and REE values (ppm) for fresh (F), highly altered - highly argillized (HAl - HAr) samples of the well 18/97.

Sample Name	18/97 -12	18/97 -14	18/97 -130	18/97 -213	18/97 -216	18/97 -418	18/97 -446	18/97 -510	18/97 -695
Alteration	HAl - HAr	F	F	HAl - HAr	F	HAl - HAr	F	HAl - HAr	F
Depth	9-10.5	11.2-11.5	81.3-82	138.5-139	149 -150	284.5-285.5	301.5-302.5	337.6-338.2	459.4-460.3
SiO_2	50.76	56.81	54.97	53.81	48.05	50.20	51.53	53.89	53.68
Al_2O_3	17.68	18.60	19.65	19.27	19.75	17.99	22.20	21.26	21.66
Fe_2O_3	4.12	3.55	7.31	5.47	5.66	4.62	6.26	6.60	6.87
Na_2O	1.77	2.21	7.17	2.89	3.41	5.44	3.07	5.17	9.18
K_2O	5.69	6.16	4.48	7.56	4.55	5.15	5.52	5.08	4.93
CaO	8.56	4.46	1.20	4.16	8.28	5.00	3.88	2.78	1.27
MgO	0.64	0.36	0.52	0.60	0.48	1.17	0.90	0.57	0.31
MnO	0.30	0.15	0.22	0.20	0.19	0.15	0.13	0.11	0.08
TiO_2	0.19	0.14	0.41	0.30	0.21	0.17	0.12	0.17	0.10
P_2O_5	0.10	0.10	0.10	0.10	0.10	0.10	0.10	0.10	0.10
A.Z	9.87	7.12	3.62	5.18	8.00	7.19	6.06	4.02	1.71
Y	50.34	73.47	82.76	114.83	241.27	14.48	7.58	7.85	4.46
La	405.73	403.68	273.51	487.56	436.89	13.75	24.23	20.76	10.21
Ce	435.02	364.45	460.18	895.21	789.19	25.25	36.34	36.81	17.78
Pr	24.22	21.79	35.61	84.69	72.74	2.51	3.19	3.47	1.85
Nd	58.45	52.48	105.32	220.94	193.81	8.46	9.40	10.86	4.25
Sm	5.59	5.68	14.89	29.40	27.82	1.93	1.38	1.60	0.76
Eu	1.03	1.11	2.97	5.49	5.57	0.59	0.29	0.36	0.17
Gd	8.27	8.43	18.94	33.75	34.36	2.36	1.79	2.01	0.82
Tb	0.77	0.98	2.39	3.76	4.63	0.38	0.24	0.25	0.13
Dy	4.49	7.03	11.96	19.93	31.30	2.18	1.15	1.50	0.71
Ho	0.95	1.61	2.90	3.42	6.66	0.55	0.29	0.32	0.15
Er	3.21	5.90	7.17	9.48	21.80	1.39	0.77	0.84	0.45
Tm	0.41	0.81	1.16	0.98	2.75	0.22	0.15	0.17	0.10
Yb	2.37	4.70	5.22	4.66	13.70	0.94	0.94	0.89	0.62
Lu	0.23	0.44	0.65	0.41	1.26	0.12	0.17	0.15	0.11
Sc	0.10	0.28	0.31	0.10	0.55	0.10	0.10	0.10	0.10
ΣREEO	1001.15	952.81	1025.95	2251.33	2227.46	75.19	88.02	87.93	42.68
Th	91.15	117.06	31.84	276.28	184.34	5.64	8.55	10.30	4.33
U	6.26	20.38	27.32	41.45	50.35	38.82	15.35	30.71	6.24
Ta	5.25	8.87	19.22	20.46	21.00	5.03	5.41	13.87	2.25
Zr	528.86	1396.85	1429.63	426.03	1701.68	87.03	424.58	412.09	258.50
Cs	8.16	3.14	43.18	4.80	5.66	1.35	4.62	22.59	18.72
Hf	3.75	7.73	12.28	4.33	13.46	1.10	4.34	5.17	4.57
Nb	250.70	322.84	337.22	535.28	495.48	120.36	100.63	226.97	39.76
Rb	412.68	469.05	416.96	502.52	429.93	177.57	270.88	176.37	252.02
Be	25.09	12.76	9.08	4.16	6.83	2.94	8.99	7.88	4.30
Ge	0.67	0.64	1.61	2.03	2.03	0.63	1.05	1.49	0.37
Ga	47.39	42.46	61.38	65.85	60.06	55.10	55.96	45.97	31.49
As	45.84	31.50	423.79	117.26	87.21	48.13	22.48	37.48	94.78
Ni	9.26	6.31	2.29	27.20	5.68	6.24	3.01	3.08	4.91
Co	0.87	0.60	0.83	0.98	0.62	0.96	0.47	0.59	0.70
Li	135.24	200.05	318.87	71.70	105.15	51.13	200.76	146.99	69.93
Bi	0.42	0.34	2.70	2.30	1.35	0.99	0.66	1.97	2.53
Cr	10.57	10.75	15.51	22.66	43.82	49.03	32.77	18.44	15.71
V	16.75	16.58	25.64	21.28	22.58	28.12	27.49	23.28	5.50
W	10.00	10.00	10.00	10.00	10.00	10.00	10.00	10.00	10.00
Sr	98.73	58.09	180.23	53.62	162.93	64.67	114.34	107.24	77.42
Ba	436.40	368.66	36.65	452.66	561.38	683.34	79.92	61.41	15.29
Sn	10.00	10.00	17.73	14.85	18.48	10.00	14.21	16.27	13.39
Cd	0.44	0.47	0.82	0.41	0.46	2.75	0.39	0.62	0.30
Cu	2.79	1.96	4.79	8.13	2.03	15.10	3.51	3.53	2.48
Pb	69.34	59.96	384.62	31.35	22.46	333.90	17.51	28.65	7.23
Zn	252.47	209.69	323.34	153.88	137.07	1328.96	106.66	223.79	76.77
Mo	2.12	1.53	2.14	4.14	3.61	4.70	3.25	2.41	2.23
Sb	2.10	1.71	3.91	3.47	9.13	1.94	1.15	2.63	1.07
ΣLREE	923.41	842.39	874.62	1717.79	1520.46	49.96	73.16	71.89	34.09
ΣHREE	7.16	13.45	17.10	81.88	122.03	3.22	2.33	2.38	1.44
Eu/Eu*	0.46	0.49	0.54	0.53	0.55	0.84	0.57	0.61	0.64
$(La/Yb)_N$	115.66	57.97	35.36	70.52	21.49	9.87	17.31	15.65	11.11
$(La/Sm)_N$	45.70	44.71	11.56	10.43	9.88	4.49	11.05	8.17	8.47
$(Ce/Yb)_N$	47.58	20.08	22.82	49.68	14.90	6.95	9.96	10.65	7.42
$(Ce/Sm)_N$	18.80	15.48	7.46	7.35	6.85	3.16	6.36	5.56	5.65
$(Eu/Yb)_N$	1.23	0.67	1.62	3.35	1.16	1.77	0.88	1.14	0.76

* REE's are normalized according to Boynton (1984).

Table 6- Major oxide, trace and REE values (ppm) for fresh (F), highly altered - highly argillized (HAl - HAr) samples of the well 18/113.

Sample Name	18/113-91	18/113-96	18/113-149	18/113-360	18/113-404	18/113-585	18/113-635	18/113-666	18/113-760
Alteration	F	HAl - HAr	HAl - HAr	F	HAl - HAr	F	HAl - HAr	HAl - HAr	F
Depth	65.6-66.3	67.7-68.7	94.5-95.5	234-235	258.8-259.8	372-373	396.7-397.1	413.6-414.7	476-477
SiO_2	49.49	43.62	49.26	55.00	50.10	55.80	49.40	56.00	53.90
Al_2O_3	19.00	16.73	19.54	19.50	19.50	18.10	20.30	18.90	20.20
Fe_2O_3	9.37	2.29	4.49	5.32	14.00	8.43	5.17	4.12	3.56
Na_2O	3.38	0.69	1.57	8.06	3.78	7.95	2.99	3.11	10.70
K_2O	3.73	7.27	7.29	5.11	3.89	3.95	5.19	4.64	4.89
CaO	6.60	15.03	8.21	2.20	2.41	2.38	7.52	4.62	1.98
MgO	0.42	0.55	0.63	0.26	1.10	0.31	0.65	0.81	0.20
MnO	0.07	0.15	0.07	0.11	0.10	0.06	0.09	0.11	0.09
TiO_2	0.24	0.21	0.38	0.13	0.36	0.12	0.19	0.13	0.08
P_2O_5	0.10	0.10	0.10	0.10	0.10	0.10	0.10	0.10	0.10
A.Z	4.37	10.98	7.73	4.10	4.15	2.78	8.09	7.34	3.91
Y	21.35	155.81	30.37	31.81	81.79	4.40	115.60	51.00	10.12
La	78.63	203.35	75.48	78.43	318.86	11.08	158.89	100.85	14.76
Ce	133.95	252.35	95.86	121.72	519.76	20.44	261.37	166.63	33.13
Pr	11.38	17.17	7.14	9.76	47.05	1.95	23.77	13.64	3.25
Nd	28.89	39.89	16.64	23.84	122.52	5.17	60.94	34.68	9.82
Sm	4.56	7.39	2.78	3.84	19.72	0.90	11.29	6.25	2.10
Eu	0.90	1.70	0.62	0.82	3.85	0.19	2.38	1.35	0.47
Gd	6.76	13.99	5.10	5.82	22.16	1.15	15.11	8.69	3.06
Tb	0.72	2.20	0.59	0.67	2.99	0.14	2.33	1.25	0.41
Dy	3.92	17.66	3.98	4.12	18.16	0.77	16.54	8.45	2.60
Ho	0.80	4.75	0.96	0.90	3.54	0.16	3.90	1.93	0.56
Er	2.34	18.45	3.37	2.84	10.14	0.54	13.02	6.59	1.62
Tm	0.29	3.21	0.53	0.38	1.09	0.10	1.86	1.04	0.22
Yb	1.49	19.57	3.38	2.08	5.11	0.66	10.01	6.26	1.33
Lu	0.17	2.04	0.38	0.22	0.44	0.10	1.00	0.64	0.15
Sc	0.10	0.94	0.12	0.10	0.10	0.10	0.26	0.10	0.10
ΣREEO	296.25	760.43	247.31	287.36	1177.28	47.85	698.28	409.35	83.67
Th	32.81	40.99	49.61	63.63	101.12	5.85	51.41	56.84	2.47
U	7.34	83.21	21.44	14.94	22.65	4.43	9.06	14.93	18.34
Ta	7.30	37.01	19.78	5.74	12.27	1.05	10.28	6.10	4.51
Zr	256.01	3190.25	1085.28	312.64	495.22	176.13	1163.61	546.64	344.99
Cs	1.56	2.43	10.06	6.73	3.90	23.54	20.33	17.78	12.05
Hf	3.65	32.93	11.86	3.13	6.71	2.90	10.48	5.10	3.07
Nb	130.33	447.10	395.43	147.42	238.86	17.80	253.82	172.76	126.05
Rb	195.35	413.13	258.75	278.88	245.81	177.05	254.91	229.94	150.81
Be	2.19	1.82	6.07	7.85	8.02	1.76	2.74	3.84	7.54
Ge	0.87	0.80	0.61	0.79	1.52	0.88	1.41	0.80	0.69
Ga	36.30	34.27	36.58	30.16	41.22	26.99	35.23	31.31	32.39
As	37.78	113.27	96.49	101.52	632.54	22.31	36.05	40.98	45.11
Ni	2.03	5.11	1.89	2.79	6.20	0.81	2.72	5.42	8.14
Co	0.23	0.92	0.38	0.60	0.32	0.21	0.38	0.43	0.52
Li	162.79	123.08	108.85	163.52	163.49	55.38	277.19	124.23	85.30
Bi	7.23	8.78	0.77	0.37	0.86	0.53	1.87	1.18	0.36
Cr	18.62	20.10	20.28	63.15	42.54	28.23	32.43	28.91	29.12
V	15.15	16.37	17.93	22.92	15.64	22.43	25.17	17.71	21.55
W	10.00	10.00	10.00	10.00	10.00	10.00	10.00	10.00	10.00
Sr	130.59	33.55	43.26	155.58	319.61	79.81	62.51	72.03	52.26
Ba	31.75	28.41	149.35	227.38	29.81	73.81	45.98	71.25	20.22
Sn	13.90	14.33	15.16	10.00	21.49	10.89	10.00	10.00	10.00
Cd	0.44	0.54	0.35	0.35	0.61	0.31	0.25	0.24	0.27
Cu	2.26	19.82	3.00	4.16	3.00	1.62	1.79	2.16	2.35
Pb	92.56	61.20	11.09	51.28	67.85	7.15	5.54	41.17	26.70
Zn	10.00	10.00	10.00	10.00	180.98	58.15	75.99	147.91	175.12
Mo	0.69	0.43	1.05	2.26	0.67	0.41	1.11	0.82	2.87
Sb	2.99	4.77	4.06	3.28	2.60	1.31	9.62	4.29	4.91
ΣLREE	252.85	512.75	195.12	233.75	1008.19	38.65	504.97	315.80	60.949
ΣHREE	5.09	48.00	8.63	6.43	20.32	1.56	29.79	16.46	3.871
Eu/Eu*	0.5	0.51	0.51	0.53	0.56	0.58	0.56	0.56	0.56
$(La/Yb)_N$	35.53	7.01	15.05	25.38	42.09	11.37	10.7	10.87	7.47
$(La/Sm)_N$	10.85	17.32	17.08	12.86	10.17	7.73	8.85	10.15	4.42
$(Ce/Yb)_N$	23.22	3.34	7.33	15.11	26.33	8.05	6.75	6.89	6.44
$(Ce/Sm)_N$	7.09	8.25	8.32	7.66	6.36	5.47	5.59	6.44	3.81
$(Eu/Yb)_N$	1.72	0.25	0.52	1.12	2.14	0.84	0.68	0.62	1

* REE's are normalized according to Boynton (1984).

Table 7- Major oxide, trace and REE values (ppm) for fresh (F), highly altered - highly argillized (Hal-HAr) samples of the well 18/114.

Sample Name	18/114-68	18/114-111	18/114 -271	18/114 -287	18/114 -392	18/114 -396	18/114 -665	BS18/114 -679
Alteration	Hal-HAr	F	Hal-HAr	F	F	Hal-HAr	Hal-HAr	F
Depth	39.7-40.2	69.5-70.5	169-170.2	178.7-179.1	249-249.7	251-251.4	438-439	448-449
SiO_2	48.13	51.70	57.02	55.67	46.30	50.99	55.91	51.60
Al_2O_3	23.37	21.02	18.65	18.73	20.64	23.77	21.42	21.09
Fe_2O_3	6.15	5.47	5.76	4.58	3.48	4.22	2.85	4.72
Na_2O	0.47	8.15	7.00	8.15	5.31	8.18	4.02	9.19
K_2O	3.05	5.05	6.32	5.33	6.45	5.50	6.82	4.84
CaO	6.11	2.75	1.58	1.90	8.68	1.97	3.40	3.01
MgO	1.50	0.61	0.47	0.23	0.45	0.21	0.62	0.35
MnO	0.21	0.20	0.12	0.17	0.18	0.07	0.07	0.11
TiO_2	0.30	0.19	0.35	0.19	0.17	0.14	0.06	0.17
P_2O_5	0.10	0.10	0.10	0.10	0.10	0.10	0.10	0.10
A.Z	9.55	3.31	2.21	4.67	7.92	4.76	4.66	4.62
Y	70.41	49.03	35.44	23.27	139.95	54.00	13.54	21.93
La	307.05	238.49	75.45	121.05	410.29	173.10	29.04	57.58
Ce	875.55	352.80	119.92	197.85	657.37	267.87	50.19	96.54
Pr	34.54	26.19	9.07	17.44	50.04	19.29	4.30	8.01
Nd	92.46	69.56	21.14	40.15	129.81	48.77	11.88	21.61
Sm	14.54	9.20	3.39	5.28	19.86	7.83	2.24	3.81
Eu	2.58	1.59	0.63	1.08	3.70	1.51	0.53	0.85
Gd	17.99	9.67	4.12	5.03	20.11	8.23	2.34	4.03
Tb	2.08	1.15	0.62	0.64	2.68	1.17	0.38	0.56
Dy	12.00	6.49	4.72	3.58	17.85	8.06	2.51	3.38
Ho	2.42	1.45	1.06	0.76	3.51	1.59	0.52	0.65
Er	6.85	4.70	3.88	2.43	12.14	5.27	1.74	1.93
Tm	0.83	0.70	0.64	0.35	1.49	0.64	0.23	0.23
Yb	3.40	3.44	4.30	2.06	8.74	3.76	1.51	1.41
Lu	0.35	0.43	0.40	0.24	0.80	0.34	0.14	0.13
Sc	0.10	0.10	0.10	0.10	0.29	0.17	0.10	0.10
ΣREEO	1443.14	774.99	284.88	421.28	1478.63	601.61	121.19	222.74
Th	135.03	167.42	40.43	75.50	159.17	97.77	36.52	34.20
U	10.00	50.73	72.50	19.01	30.92	18.31	1.54	15.32
Ta	12.52	9.89	35.59	12.72	18.94	9.12	5.10	6.92
Zr	363.19	964.39	1377.78	580.10	826.47	369.73	131.86	268.98
Cs	8.93	22.09	6.85	13.42	13.00	22.52	22.32	24.49
Hf	4.60	7.84	12.63	6.72	7.03	4.02	2.20	3.91
Nb	262.46	225.34	853.97	275.18	496.27	259.90	97.62	146.45
Rb	362.11	273.39	313.22	134.31	457.29	526.96	304.44	218.38
Be	3.66	11.79	7.72	16.33	15.96	15.00	6.22	9.50
Ge	1.46	0.98	0.79	0.90	1.60	1.72	0.88	0.80
Ga	73.42	48.48	49.49	34.06	57.62	66.28	41.71	34.03
As	147.01	56.77	111.32	76.52	489.10	404.18	34.64	33.53
Ni	38.48	1.66	0.79	0.74	3.36	3.28	2.62	2.46
Co	4.65	0.65	0.10	0.64	1.28	0.98	0.25	0.40
Li	189.00	235.14	124.27	257.08	398.24	396.68	150.09	147.68
Bi	3.17	1.82	0.54	1.00	2.66	2.46	1.07	0.83
Cr	5.34	30.22	17.91	12.21	17.52	29.90	12.30	16.74
V	15.54	20.15	25.68	10.69	38.41	36.25	21.79	18.33
W	10.00	10.00	10.00	10.00	10.00	10.00	10.00	10.00
Sr	52.62	380.20	63.57	72.82	472.20	316.31	53.65	129.53
Ba	1142.85	455.71	111.45	314.23	483.99	420.27	127.15	26.02
Sn	18.21	12.35	14.24	10.00	12.82	15.16	10.00	10.00
Cd	0.51	0.90	0.10	0.41	0.73	0.55	0.25	0.35
Cu	12.86	2.36	0.10	0.46	3.30	5.17	2.32	2.64
Pb	83.50	91.24	264.33	93.65	150.04	158.61	22.03	46.40
Zn	306.03	575.95	572.39	362.26	432.47	340.17	136.88	388.80
Mo	3.61	3.84	1.06	1.52	2.42	3.41	1.76	2.21
Sb	7.10	3.06	2.50	5.93	11.14	7.04	4.49	2.61
ΣLREE	1309.60	687.04	225.57	376.48	1247.52	509.02	95.42	183.74
ΣHREE	25.84	17.20	15.00	9.41	44.53	19.67	6.64	7.71
Eu/Eu*	0.49	0.52	0.52	0.64	0.57	0.58	0.71	0.66
$(La/Yb)_N$	60.81	46.69	11.84	39.62	31.67	31.02	12.99	27.61
$(La/Sm)_N$	13.29	16.3	13.98	14.43	13	13.91	8.14	9.5
$(Ce/Yb)_N$	66.53	26.5	7.22	24.84	19.47	18.42	8.61	17.76
$(Ce/Sm)_N$	14.54	9.25	8.53	9.05	7.99	8.26	5.4	6.11
$(Eu/Yb)_N$	2.15	1.32	0.42	1.48	1.2	1.14	1	1.72

* REE's are normalized according to Boynton (1984).

Table 8- Major oxide, trace and REE values (ppm) for fresh (F), highly altered - highly argillized (Hal-HAr) samples of the well 18/151.

Sample Name	18/151 -179	18/151 -205	18/151 -225	18/151 -306	18/151 -331	18/151 -469	18/151 -659	18/151 -722
Alteration	Hal-HAr	Hal-HAr	F	F	Hal-HAr	F	Hal-HAr	F
Depth	131-132	144.8-145.6	159-160	211-212	228.3-229.7	299-300	426-427	478.3-479
SiO_2	47.57	57.10	55.30	55.80	52.20	52.80	52.70	54.30
Al_2O_3	20.89	19.40	19.20	20.10	20.30	19.80	19.70	22.10
Fe_2O_3	7.65	5.61	4.59	4.53	8.12	5.38	3.19	2.20
Na_2O	1.48	3.15	8.74	7.94	3.96	3.72	2.62	5.33
K_2O	1.14	6.43	5.15	5.22	2.82	5.04	7.17	6.36
CaO	8.37	2.10	1.50	2.26	4.50	4.90	5.40	2.98
MgO	1.64	0.87	0.76	0.75	0.93	1.05	1.16	0.75
MnO	0.43	0.29	0.24	0.15	0.16	0.09	0.08	0.05
TiO_2	0.39	0.31	0.19	0.17	0.22	0.20	0.15	0.06
P_2O_5	0.10	0.10	0.10	0.10	0.10	0.10	0.10	0.10
A.Z	9.43	3.88	3.89	2.73	6.49	6.83	7.61	5.62
Y	202.80	111.08	61.97	19.14	34.16	9.77	22.71	12.79
La	589.06	414.66	268.83	119.00	103.57	16.21	35.97	23.44
Ce	1173.72	685.83	384.55	219.63	203.07	29.96	61.64	47.41
Pr	85.61	51.75	26.33	16.38	13.12	2.35	5.79	4.02
Nd	228.88	132.68	60.52	39.71	31.18	5.84	16.00	10.86
Sm	37.84	21.02	8.07	4.94	5.02	0.99	3.12	1.87
Eu	6.66	4.29	1.62	1.00	1.07	0.21	0.73	0.44
Gd	42.12	22.30	9.18	4.96	5.83	1.68	4.18	2.01
Tb	5.10	3.12	1.28	0.57	0.83	0.18	0.56	0.33
Dy	34.90	16.80	7.41	2.78	4.79	1.14	3.64	1.84
Ho	6.15	3.83	1.82	0.62	1.10	0.26	0.80	0.43
Er	20.00	10.68	5.58	1.83	2.97	0.85	2.50	1.17
Tm	2.27	1.57	0.86	0.30	0.40	0.12	0.38	0.17
Yb	11.79	7.82	4.24	1.77	1.96	0.72	2.19	0.79
Lu	1.03	0.81	0.43	0.22	0.21	0.10	0.25	0.10
Sc	0.16	0.10	0.10	0.10	0.10	0.10	0.10	0.10
ΣREEO	2448.09	1488.34	842.77	432.94	409.38	70.49	160.54	107.77
Th	337.15	244.22	135.51	51.96	35.36	15.50	16.48	6.53
U	28.58	52.03	39.58	26.48	9.27	22.56	59.62	4.08
Ta	23.91	22.49	9.65	7.85	4.05	6.40	11.61	1.44
Zr	1331.40	1343.38	377.91	278.11	266.21	175.11	241.43	40.79
Cs	4.55	10.02	17.76	7.22	16.23	5.18	25.06	26.63
Hf	12.15	12.36	3.96	3.34	3.82	2.48	3.11	0.45
Nb	651.70	519.29	199.64	136.77	84.08	190.76	154.71	22.52
Rb	125.75	248.29	210.93	157.30	202.35	192.72	246.96	85.28
Be	17.94	16.15	16.15	4.77	4.60	6.15	5.40	1.78
Ge	1.33	0.74	0.38	0.42	0.53	0.99	0.78	0.30
Ga	69.69	37.66	35.37	24.84	40.54	39.39	30.91	13.16
As	47.53	155.81	59.96	41.03	314.44	23.30	26.83	13.35
Ni	61.19	3.05	1.81	2.02	12.86	1.86	4.43	1.46
Co	5.02	0.48	0.48	0.43	0.86	0.25	0.50	0.25
Li	712.89	491.87	361.22	89.01	125.57	222.95	133.59	69.73
Bi	1.10	0.95	0.60	0.56	2.10	4.74	1.37	1.09
Cr	5.49	5.99	6.86	12.75	4.73	12.28	4.71	14.47
V	15.69	13.59	12.27	13.34	11.33	34.68	21.75	15.79
W	10.00	10.00	10.00	10.00	10.00	10.00	10.00	10.00
Sr	126.33	126.27	192.96	236.34	166.09	115.48	94.35	79.62
Ba	496.60	585.61	367.78	358.39	637.62	24.94	154.11	71.10
Sn	20.12	11.06	10.00	10.00	11.96	10.00	10.00	10.00
Cd	1.27	0.61	0.36	0.39	0.68	0.24	0.22	0.12
Cu	5.57	4.31	2.89	2.40	2.91	1.17	2.63	1.52
Pb	570.79	314.23	68.86	107.76	123.55	9.94	32.09	5.66
Zn	773.63	607.28	299.15	128.76	179.38	56.19	98.85	66.02
Mo	2.06	1.60	2.00	1.53	1.14	0.91	1.19	2.80
Sb	3.42	4.33	5.28	1.31	2.16	2.56	0.10	1.12
ΣLREE	2077.27	1284.92	740.23	394.72	350.95	54.36	119.40	85.74
ΣHREE	41.24	24.71	12.92	4.73	6.64	2.06	6.11	2.66
Eu/Eu*	0.51	0.61	0.58	0.62	0.6	0.49	0.61	0.69
$(La/Yb)_N$	33.68	35.77	42.78	45.45	35.68	15.16	11.08	19.98
$(La/Sm)_N$	9.79	12.41	20.96	15.14	12.98	10.27	7.25	7.88
$(Ce/Yb)_N$	25.75	22.7	23.48	32.19	26.84	10.75	7.29	15.5
$(Ce/Sm)_N$	7.49	7.87	11.5	10.72	9.76	7.28	4.77	6.12
$(Eu/Yb)_N$	1.61	1.56	1.09	1.61	1.55	0.81	0.94	1.57

* REE's are normalized according to Boynton (1984).

69 (Table 4), 5 T, 4 İB - İK from BS18 - 97 (Table 5), 4 T, 5 İB - İK from BS18 - 113 well (Table 6), 4 T, 4 IB – IK from well BS18 - 114 (Table 7), 4 T and 4 İB - İK samples from well BS18 - 151 (Table 8) (total of 66) were taken. The REE totals (ΣREEO) of the samples in well 17/59 are higher at all levels of the drilling than T and B - K at the highly altered - highly argillized levels. Thorium (Th) values are higher at depths close to the surface than at the bottom of the well. Niobium (Nb) values are higher at depths close to the surface and lower at deeper parts of the well. Lead (Pb) and Zinc (Zn) values are higher at depths close to the surface than at the bottom of the well (Table 1). In well 17/65, the values of ΣREEO, Zr, Nb, Rb, Lithium (Li) elements in the middle depths of the well are higher than the bottom and top of the well. Barium (Ba) and Strontium (Sr) values are higher at the bottom of the well (Table 2). In well 17/67, the values of ΣREEO, Nb, U, Th, Zr, Rb, Li, Ba, Pb, Zn elements are higher throughout the depth of the well compared to the T at highly altered - highly argillized levels. In well 17/69, the ΣREEO, Nb, Th, Zr, Rb, Ba, Pb, Zn elements reach higher values in the İB - İK, while Li and Sr elements reach higher values in the T. In well 18/97, ΣREEO and Ba elements are higher in the İB - İK compared to the T, however, Nb, Zr, Li, Rb elements are higher in the T compared to the İB - İK. In well 18/113, the ΣREEO, Nb, Zr, Rb, Li elements are higher in the İB - İK compared to the T. In well 18/114, ΣREEO, Th, Zr, Ba elements are higher in the IB – IK compared to the T, while Nb, Rb elements are higher in the T compared to İB - İK. In well 18/151, ΣNYEO, Nb, Th, Zr, Rb, Li, Ba, Pb, Zn elements are higher in the İB - İK, and Sr element is higher in the T than İB - İK.

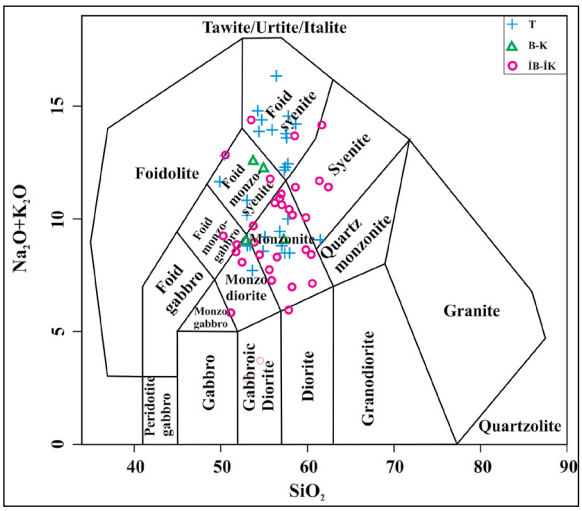

Figure 5- Rock classification according to Middlemost (1985). T: fresh, B - K: altered - argillized, İB - İK: highly altered - highly argillized.

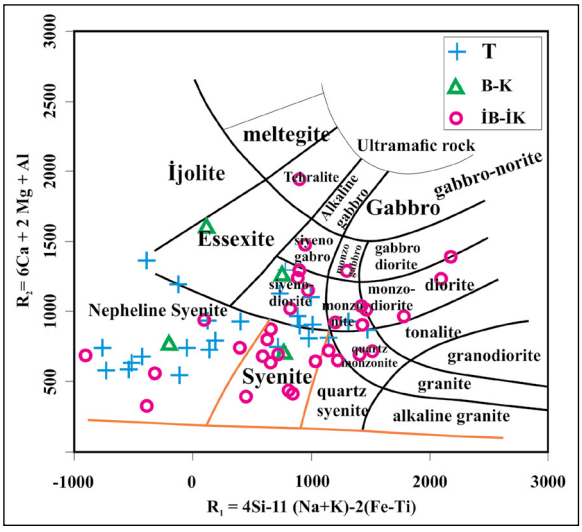

Figure 6- Rock classification according to R1-R2 De La Roche et al. (1980). The symbols are the same in Figure 5.

5.2. Classification of Magmatic Rocks

Middlemost (1985)'s SiO_2 - Na_2O - K_2O diagram was drawn as named T, B - K, and İB - İK (Figure 5). The T fall into foid syenite, foid monzo syenite, monzodiorite, and syenite area, the B - K fall into foid monzo syenite, monzonite, monzodiorite area, the İB - İK fall into foid syenite, syenite, monzonite, monzo gabbro diorite area (Figure 5). In R1 - R2 De La Roche et al. (1980) diagram in Figure 6, the T fall into nepheline syenite, syenite, syenodiorite, monzonite, quartz monzonite, quartz syenite, gabbro, and diorite area, the B - K fall into nepheline syenite, syenite, essexite and syenodiorite area, and the İB - İK fall into the nepheline - bearing syenite, syenite, syenodiorite, monzogabbro, monzonite, quartz monzonite and monzodiorite areas. According to Shand (1943)'s A/CNK - A/NK diagram (Figure 7), the samples show both metaluminous and peraluminous composition.

5.3. Major and Trace Element Variations

The changes in the results obtained from the chemical analysis of 66 samples taken from 8 wells, depending on SiO_2 value in the study, were interpreted with Harker diagrams. As the amount of SiO_2 decreases, the amount of TiO_2, Al_2O_3, MgO, CaO, FeO increases

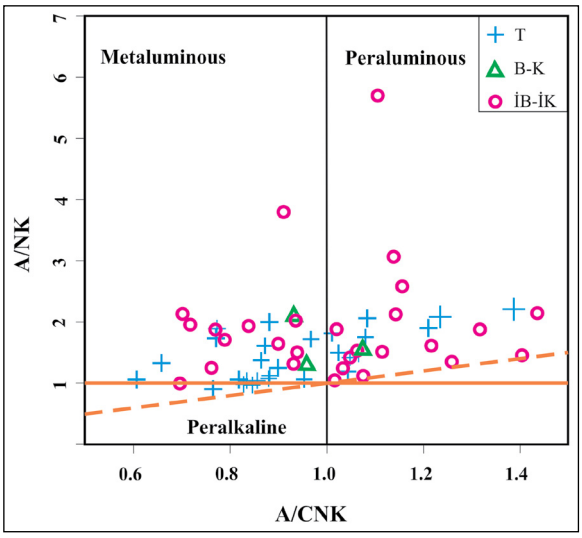

Figure 7- Classification according to Shand (1943). The symbols are the same in Figure 5.

in fresh rocks, whereas Na_2O and K_2O values decrease (Figure 8). Thus; Si, K and Na contents increase from ultramafic rock to mafic rock, while Ca, Mg, Ti, Fe decrease (Kadıoğlu, 2001). The negative orientations observed in the Harker diagrams (Figure 8) show that plagioclase, K - feldspar, amphibole, biotite, apatite, and Fe - Ti oxide minerals play an active role in fractional crystallization during rock formation.

When the changes of FeO_t and TiO_2 depending on SiO_2 are examined, it is seen that the graphs are similar to each other, and the elements such as Nb, Zr, Ta, and Tb are controlled by zircon, ilmenite, and rutile. The positive orientation of the Rb element is consistent with the crystallization of the hornblende mineral (Figure 8). The negative change in the Sr element is compatible with the crystallization of plagioclase minerals. The trace element Harker diagrams are shown in Figure 9.

5.4. Incompatible Element and REE Distributions

Figures 10 and 11 show trace element spider diagrams of the studied samples normalized to the primary mantle (Sun and Mc Donough, 1989) and chondrite (Boynton, 1984). Accordingly, it is seen that the T is generally depleted in terms of Ba, Nb, La, Ce, Ti, Y, Yb elements and enriched in terms of U, K, Pb, and Zr. Generally, the depletion in Ba, K, Ti elements and enrichment in Th, U, Nb, La, Ce, Zr, and Eu elements are observed in the İB - İK (Figure 10).

When looking at the REE chondrite normalized spider diagrams according to Boynton (1984) of the samples, enrichment in light rare earth elements (LREE) and depletion in heavy rare earth elements (HREE) are observed. Concave patterned distributions formed by REE in the spider diagram represent the alteration of hornblende and plagioclase minerals. The high slope of La and Ce elements on the graph in Figure 10 indicates that REEs are enriched at different degrees in the parent magma (Thompson et al., 1984; Thirwall et al., 1994).

6. Petrogenesis

6.1. Tectonic Setting of the Study Area

In the tectonic classification diagram created by Pearce et al. (1984) in the study area, the mid-oceanic ridge granitoids (ORG), within plate granitoids (WPG), syn - collisional granitoids (COLG), and volcanic arc granitoids (VAG) were distinguished (Figure 12). When we plot the fresh and altered samples onto these diagrams; the samples fall into the WPG area in the Rb - Y + Nb diagram in Figure 12a. Some of the T in the Nb -Y diagram fall into the VAG + syn - COLG area in Figure 12b, most of the samples fall into the WPG area in Figure 12c in the Rb - Ta + Yb diagram and some of them fall into in the syn - COLG area in Figure 12c, most of the samples fall into the WPG area in Figure 12d Ta - in the Yb diagram, and some of the fresh samples fall into the syn - COLG area in Figure 12d. Mafic rocks due to within plate magmatism are more enriched in terms of unstable elements than tholeiitic rocks. The high contamination of the crust causes within plate granites to be misclassified as volcanic arc granites or collisional granites, or rarely, for volcanic arc granites to be interpreted as syn - collisional granite. In Figure 12, the contamination effect on the crust is seen. In Figure 13, all the elements from Sr to Zr show significant anomalies and show a camel hump ridge shape (Kadıoğlu, 2001) in the MORB normalized diagram according to Pearce (1983), (Figure 13).

6.2. Interpretation of the Origin

When the results of the chemical analysis, the trace and REE analyses of the samples were plotted onto the interpretation diagram of the tectonic formation environment, it was observed that the fresh samples were generally in the syn - COLG region and the

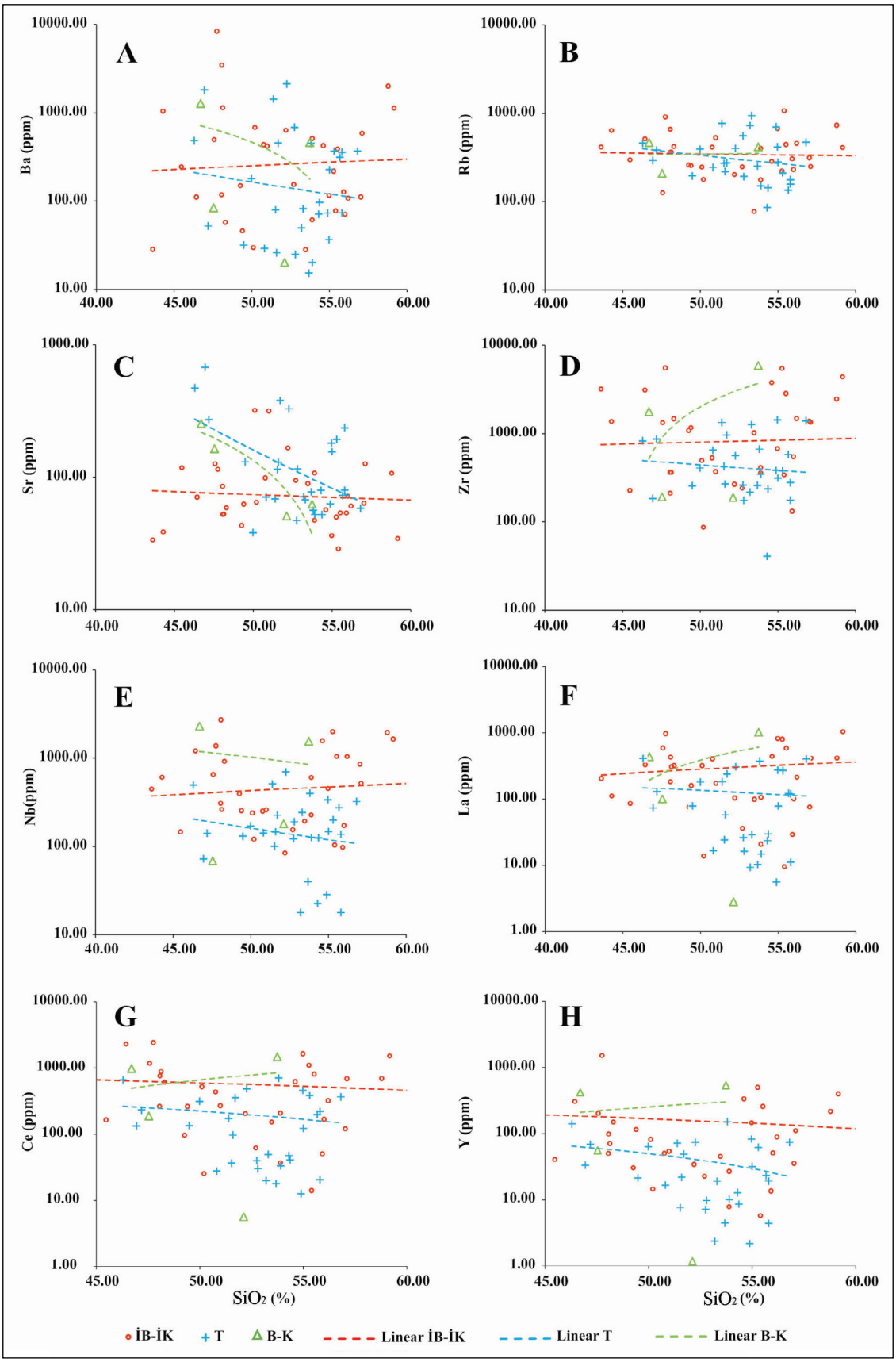

Figure 8- SiO_2 - major oxide exchange diagrams of the studied samples.

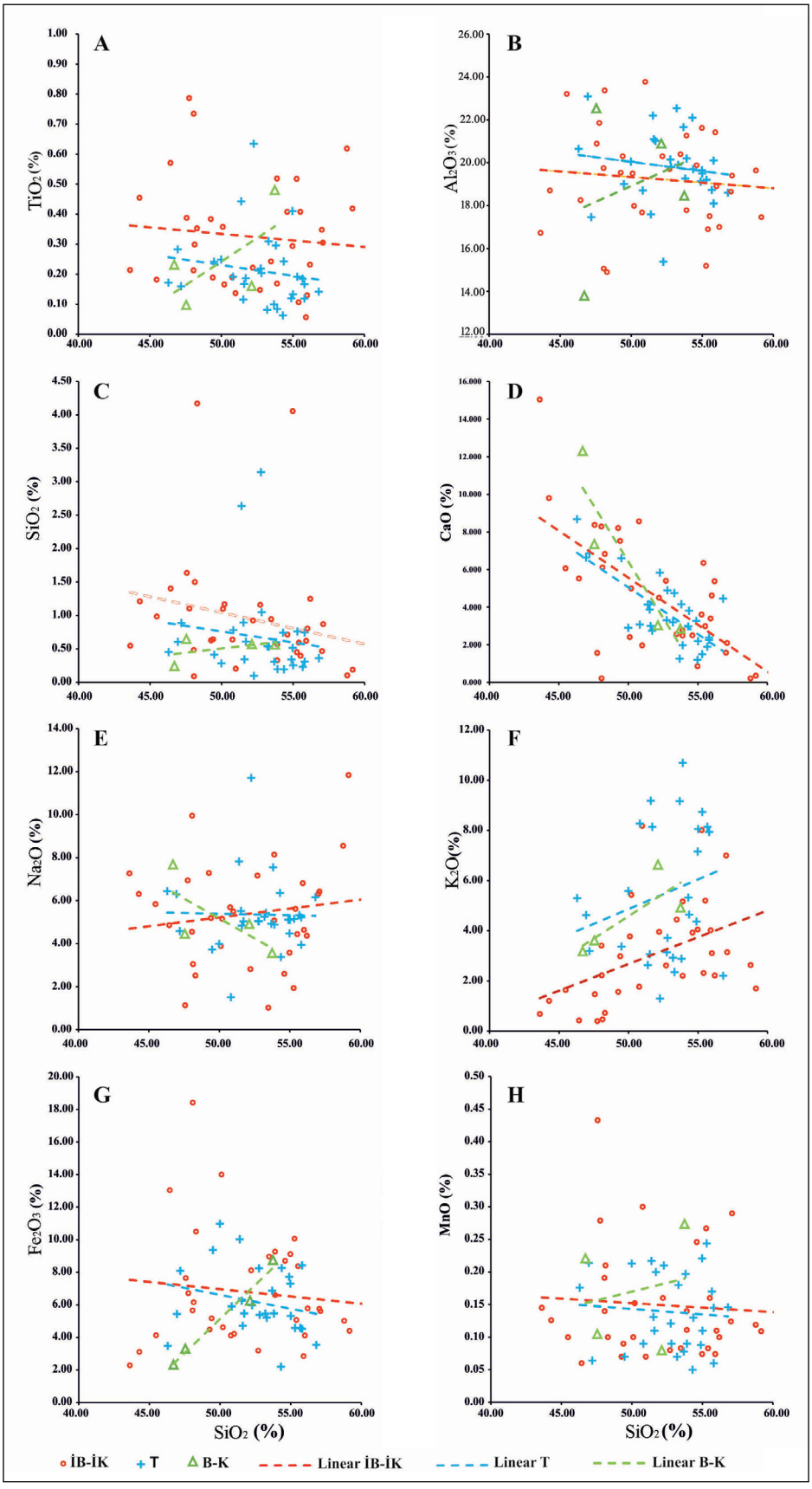

Figure 9- SiO_2 - trace element exchange diagrams of the studied samples.

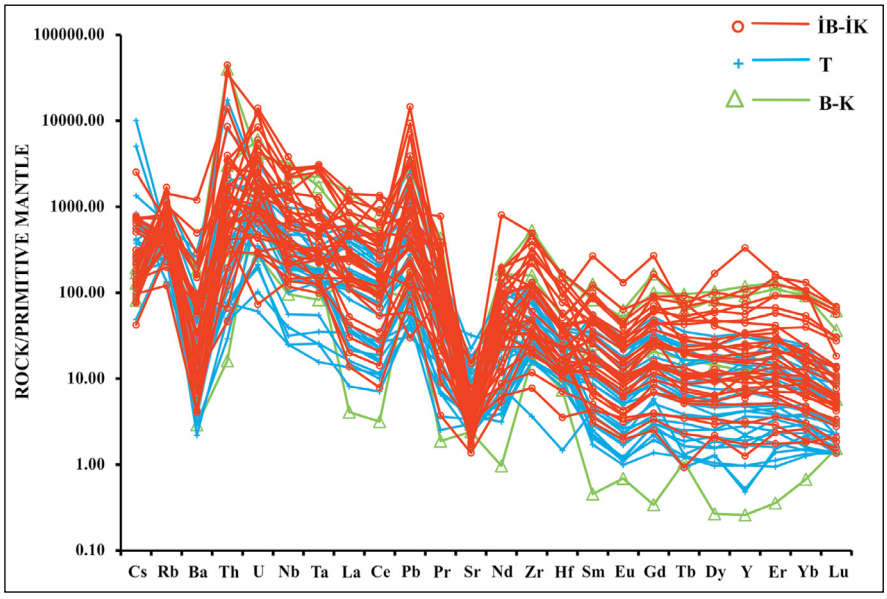

Figure 10- Spider diagram of REE according to the primary mantle (Sun and Mc Donough, 1989). The symbols are as same as in Figure 5.

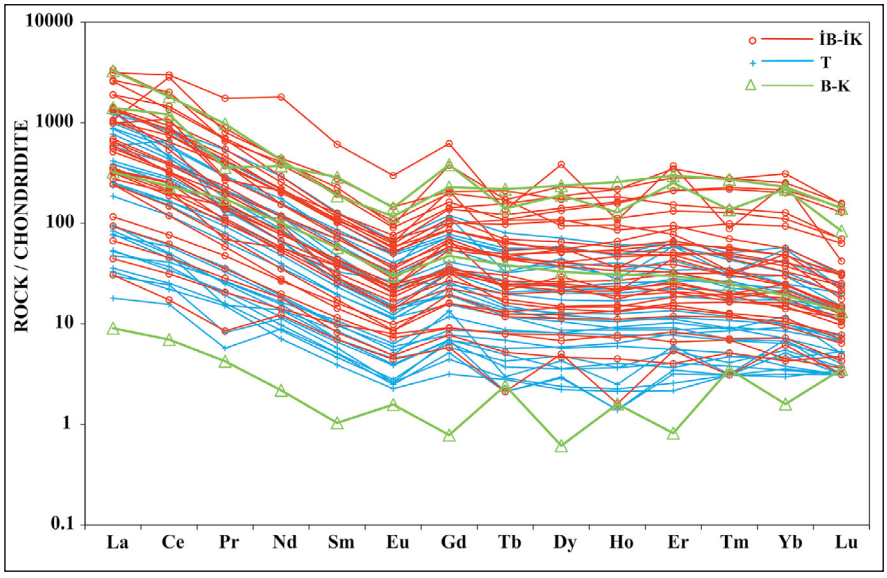

Figure 11- Spider diagram of REE according to chondrite (Boynton, (1984). The symbols are the same as Figure 5.

altered samples remained in the WPG. The positive Nb, Ta anomaly of the altered samples (Figure 12) indicates that they were formed together within plate magmatics (Altın, 2019). The negative Nb, Ta anomaly of the fresh samples indicates that these rocks are associated with a hybrid magma, which is a mixture of mantle and crust, indicating the metasomatic mantle (Altın, 2019). The thinning of the continental lithosphere facilitates decompression melting of the magma and the emplacement of a wide range of magma ranges, including the existing alkali-rich, silica-poor unsaturated rocks (carbonatite, nephelinite, and phonalite). These magmas generally settle along cracks, grabens, crustal lineaments, and large magmatic zones associated with reverse fault systems form (Chakhmouradian and Zaitsev, 2012).

It is characterized by the fact that the silica - unsaturated rocks from the environments where rifting develops are significantly enriched in light rare

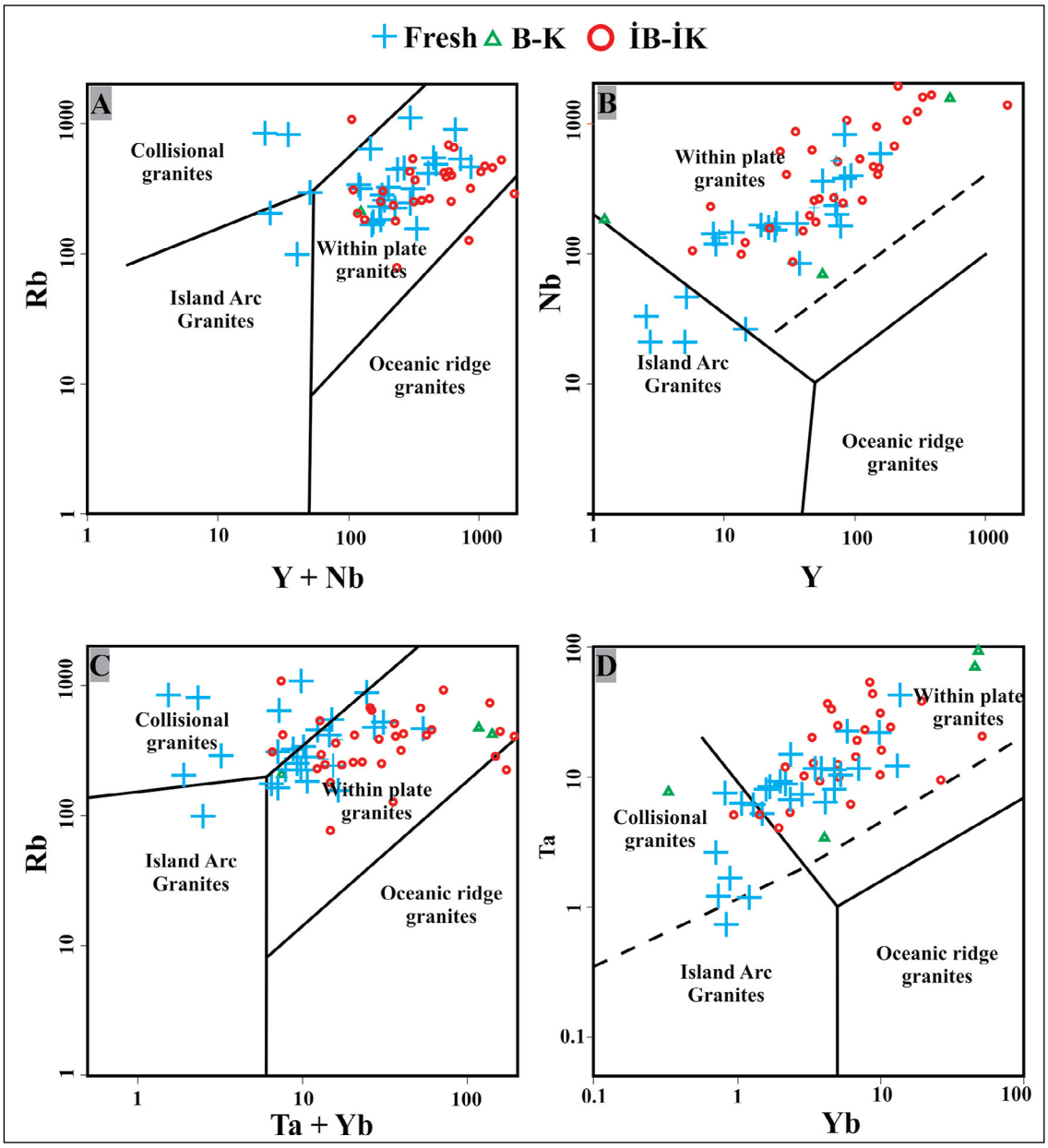

Figure 12- Tectonic classification diagram of the samples (Pearce et al., 1984). The symbols are as same as in Figure 5.

earth elements (LREE) and a higher degree of light (HLREE) - heavy fraction (HREE) characterized by [(La/Yb)] (Chakhmouradian and Zaitsev, 2012). When [(La/Yb)] values obtained from the analysis results of the samples taken from the wells are examined, it was seen that; i) in all of the wells in the study they increased from the bottom to the surface in the T, B - K and İB - İK, ii) BS17/69 located at the center of the syenite porphyry decreased towards the contact zone (from east to west) in wells BS17/59, BS17/65, BS17/67, as it moved away from the center (from east to west), iii) syenite increased in the wells BS18/97, BS18 - 113, BS18 - 114 and BS18 - 151 from west to east from syenite contact into the limestone.

In the place where syenite is emplaced, the rock is emplaced by a more gradual cooling towards the center with the effect of sudden cooling from contact metasomatism. In this mass, the increase of the [(La/Yb)] fraction from deep to the surface, and the presence of contact metasomatic effect in the wells (BS18/97, BS18 - 113, BS18 - 114, and BS18 - 151) drilled away from the syenite's contact with the limestones were observed in the cores. It was observed in the wells

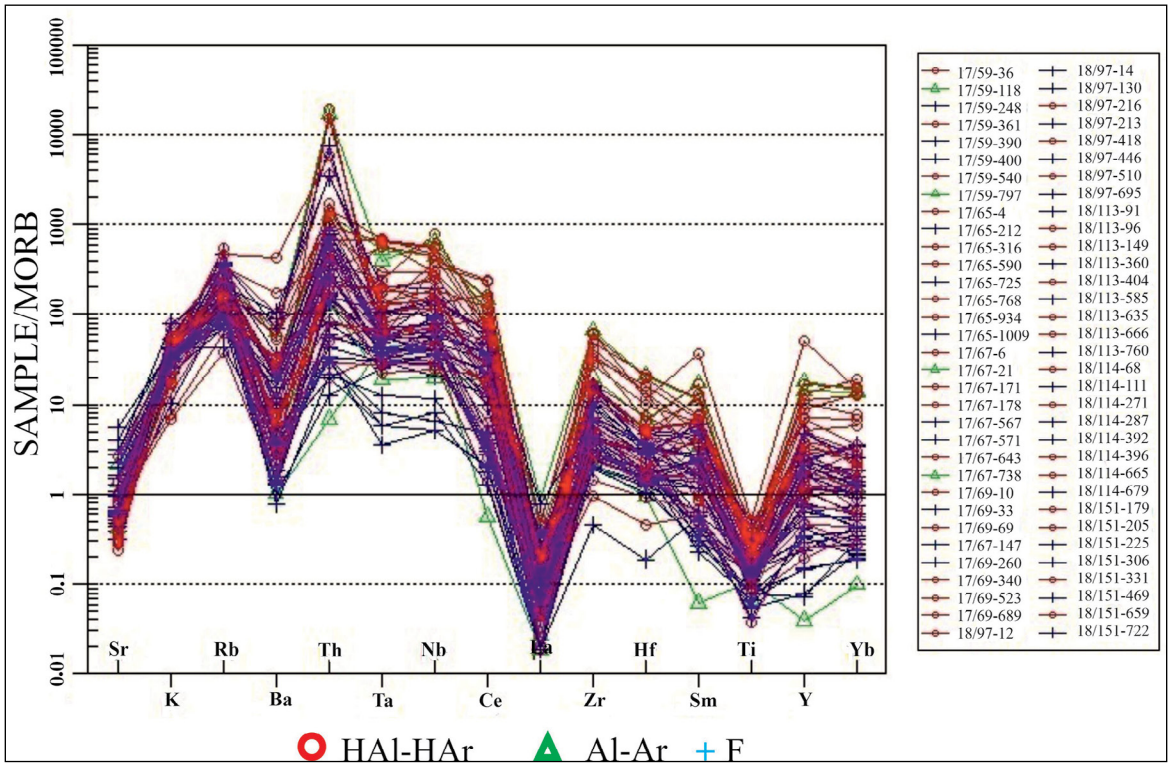

Figure 13- MORB normalized spider diagram (Pearce et al., 1984) of the samples. The symbols are as same as in Figure 5.

drilled that it had been decomposed by metasomatism under the influence of melts and fluorine-rich waters enriched in the gas phase.

The syenite below the limestone degraded the altered - argillized and highly altered - highly argillized rocks from fresh rocks in more than one phase with the effect of solutions and melts coming from deep to the surface with a certain temperature and pressure, causing their primary structures to change and become unrecognizable. It is observed with the separation of LREEs from HREEs with increasing slope and crystallization separation of feldspars and the emergence of a negative Eu anomaly in Figure 11 in the chondrite normalized diagram. This situation may cause a large increase in the rare earth element contents compared to the original magma by the fractional crystallization process and the production of advanced melts that create rare earth element mineralization. The rare earth element enrichment level required for this phenomenon to happen; depends on melt composition and physical parameters (Chakhmouradian and Zaitsev, 2012). The separation of a homogeneous melt into two or more liquids of different composition, structure, and rheology can also contribute to the rare earth element concentration in igneous systems. If one of the liquids (melt or fluid) has a lower affinity for REE than the conjugate phase value, the REE values will be enriched secondarily (Chakhmouradian and Zaitsev, 2012).

7. Discussion

The Kuluncak syenitoid was emplaced by cutting the limestones of the Domuzdağı Nappe in the study area. Özgenç and Kibici (1994) distinguished two carbonatite phases as the early phase carbonatites and late phase carbonatites. Moreover, Özgenç and İlbeyli (2009) stated that the Late Cretaceous alkaline magmatic rocks were widely found in Hasançelebi and Başören (Malatya) regions, and Başören intrusive rocks mainly contained feldspathoidic syenites cut by feldspathoidic dykes. Çimen et al. (2020) stated that the mineralization in the Kuluncak deposit is caused by the hydrothermal fluids and melt exchange is associated with magmatism after an intense collision, and is formed during metasomatism due to contact between plutonic rocks and limestones. Uras et al. (2019), in their study on Kuluncak fluorites, stated that the REE content of the Kuluncak fluorites was richer than the Yeşilyurt fluorites in terms of the Sr content. In our studies; the skarn zones were formed

and large garnet crystals were formed in places where the feldspathoidic alkaline magma cuts the limestones of the Upper Jurassic - Lower Cretaceous Domuzdağı Nappe. The skarn zones were formed by the effect of contact metamorphism, rich in intensely chloritized, epidotized phylogopite and biotite micas with high gamma radiation in some places. It is observed that the fluorite ore zones are formed with alterations indicating that the settlement of alkaline magma is located in more than one temperature and pressure phase in the field. These zones are associated with faults and secondary fractures that carry ores formed during the magma emplacement and later processes. The thickness of very coarse crystalline albites belonging to the pegmatitic phase and aegirite crystals range from 0.1 mm to 3 cm, and their lengths range from 5 cm to 10 cm. Depending on the skarn zones, both alkali and carbonate-rich mineral formations at the contact have formed the fenitized zones. With the effect of contact metasomatism, the fresh rocks contain lower REE values than the altered rocks. It was observed that the fresh rock was exposed to weathering with more than one intersecting vein system, accompanied by silicified carbonate veins that bring low-value REE and solutions rich in the REE in the hydrothermal phase. It was observed that pyrite, locally galena, sphalerite, phylogopite, and vermiculite micas were formed at low temperatures with the development of carbonate veins.

8. Results

It was observed that the fresh rock samples generally remained in the region of COLG and WPG. The positive Nb and Ta anomalies of the samples indicate that they are formed together within plate magmatic. The negative Nb and Ta anomalies of the fresh samples indicate that these rocks are related to a hybrid magma, which is a mixture of mantle and crust, indicating the metasomatic mantle. In addition, with the effect of metasomatism, it can give such distributions in low-grade partial melts in a post-collisional tectonic environment of the mantle (Çimen et al., 2020). The concave patterned distributions formed by the REE in the spider diagrams represent the alteration of hornblende and plagioclase minerals. The steep inclination of La and Ce elements on the graph indicates that the REE are enriched in different degrees in the parent magma (Altın, 2019). It is thought that this enrichment may be due to the contact metasomatism effect and solutions accompanied by silicified carbonate fluorite coming from deep (Çimen et al. 2020). It was observed that the altered samples were more enriched with the REE than the other rare metals compared to the T. It was observed that gaseous component solutions rich in fluorine and the REE coming from the bottom to the surface at different times enriched the REE at low values in the rocks. It is characterized by the fact that the silica-unsaturated rocks from the environments where rifting develop are significantly enriched in light rare earth elements (LREE) and a higher degree of light (HLREE) - heavy (HREE) fraction is characterized by [(La/Yb)] (Chakhmouradian and Zaitsev, 2012). It was seen that BS17/69 located at the center of the syenite porphyry decreased towards the contact zone (from east to west) in wells BS17/59, BS17/65, BS17/67, as it moved away from the center (from east to west). It was also observed that syenite increased in the wells BS18/97, BS18 - 113, BS18 - 114, and BS18 - 151 from west to east from the syenite contact into the limestone. The presence of some fresh samples has been observed at levels containing high levels of REE and metals. It is considered that the enrichment may be doubled or more depending on the increase in the severity of alteration and argillization of the REE.

Acknowledgements

This study was carried out within the scope of rare earth element potential and lithium explorations project of the Sofular - Kuluncak - Malatya region in the east of Anatolia between 2014 - 2018 and within the scope of the Central and Eastern Anatolia rare earth element exploration project from 2018 to recent, under the coordination of the Mineral Research and Exploration Department of the MTA General Directorate.

References

Altın, İ. 2019. Şaroluk (Gönen-Balıkesir) Granitoyidinin petrografik, jeokimyasal, ve petrolojik özellikleri. Yüksek Lisans Tezi, Balıkesir Üniversitesi, Balıkesir.

Booth, M. G., Robertson, A. H. F., Taşlı, K., İnan, N., Ünlügenç, U. C., Vincent, S. 2012. Two-stage development of the Late Cretaceous to the Late Eocene Darende Basin: implications for closure of Neotethys in central-eastern Anatolia (Turkey). Geological Society of London, Special Publications 372, 385-412.

Boynton, W. V. 1984. Geochemistry of the rare earth; meteorite studies. Henderson, P. (Ed.). Rare Earth Element Geochemistry, Elsevier, 63-114.

Camuzoğlu, M., Bağcı, U., Koepke, J., Wolff, P. E. 2017. Tectonic significance of the cumulate gabbros within Kuluncak ophiolitic suite (Malatya, SE Turkey) inferred from geochemical data. Ofioliti 42 (2), 81-103.

Camuzoğlu, M., Bağcı, U. 2018. Kuluncak ofiyolitine (Malatya, GD Türkiye) ait mafik kümülatların Sr-Nd-Pb izotop jeokimyası. 8. Jeokimya Sempozyumu, Bildiri Özleri Kitabı.

Chakhmouradian, A., Zaitsev, A. N. 2012. Rare earth mineralization in igneous rocks: sources and processes. Elements Magazine 8, 327-328.

Çimen, O., Corcoran, L., Kuebler, C., Simonetti, S., Simonetti A. 2020. Geochemical, stable (O, C, ve B) and radiogenic (Sr, Nd, Pb) isotopic data from the Eskişehir-Kızılcaören and the Malatya-Kuluncak (E-central Anatolia) F-NYE-Th deposits, Turkey: implication for nature of carbonate-hosted mineralization. Turkish Journal of Earth Sciences, TÜBİTAK.

Çobankaya, M. 2011. Hekimhan (Malatya) yöresinin Oligosen istifini sedimantolojisi. Yüksek Lisans Tezi, Ankara Üniversitesi, Fen Bilimleri Enstitüsü, Ankara.

De La Roche, H., Leterrier, J., Grandclaude, P., Marchal, M. 1980. A classification of volcanic and plutonic rocks using R1 R2-diagram and major element analyses: its relationships with current nomenclature. Chemical Geology 29, 183-210.

Dinçer, F. 2009. Darende Havzası (KB Malatya) paleojen istifinin bentik foraminiferlerinin mikropaleontolojik incelemesi ve ortamsal yorumu. Yüksek Lisans Tezi, Çukurova Üniversitesi, Fen Bilimleri Enstitüsü, Adana.

Gürer, Ö. F. 1992. Hekimhan-Hasançelebi (Malatya) dolayının jeoloji incelemesi. Doktora Tezi, İstanbul Üniversitesi, Fen Bilimleri Enstitüsü, 323.

Gürer, Ö. F. 1994. Hekimhan-Hasançelebi yöresinin üst Kretase stratigrafisi ve havza evrimi. Türkiye Jeoloji Bülteni 37(2), 135-148.

Gürer, Ö. F. 1996. Hekimhan yöresindeki alkali magmatik kayaların jeolojik ve petrolojik incelemesi. Turkish Journal of Earth Sciences 5, 71-88.

Kadıoğlu, Y. K. 2001. Mafik ve ultramafik magmatik kayaçların ana, eser ve Nye jeokimyası karakteristikleri ve jeofiziksel açıdan incelenmeleri. Magmatik Petrojenez Lisanüstü Yaz Okulu, Akçakoca.

Kuşçu, İ., Erler, A. 1998. Mineralization events in a collision-related setting the central Anatolian crystalline complex. International Geology Review, 552-565.

Kuşçu, İ., Kuşçu, G. G., Tosdal, R., Ulrich, T. D., Friedman, R. 2014. Magmatism in the southeastern Anatolian orogenic belt: transition from arc to post-collisional setting in an evolving orogen. Geological Society of London, Special Publications 2010, 437-460.

Kuru, G. S., Kuşçu, İ., Şalış, B., Yılmazer, E., Demirela, G. 2006. Hasançelebi (Malatya) demiroksit yataklarının oluşum koşulları: mikrotermometrik bir yaklaşım. Bulletin of the Mineral Research and Exploration 132, 101-111.

Marschik, R., Spikings, R., Kuşçu, I. 2008. Geochronology and stable isotope signature of alteration related to hydrothermal magnetite ores in Central Anatolia, Turkey. Mineral Depo 43,111-124.

Metin, Y., Vergili, Ö., Çörekçioğlu, E., Öcal, H., Taptık, M., Çobankaya, M., Duygu, L., Tunçdemir, V. Duran, Bağcı, S., U. Rızaoğlu, T., Uçar, L., Sevimli, U. İ. 2013. Doğu Toroslar'ın kuzey kesiminin jeodinamik evrimi, Hekimhan-Darende-Kuluncak ve çevresi. Maden Tetkik ve Arama Genel Müdürlüğü, Rapor No: 11685, 263, Ankara (unpublished).

Middlemost, E. A. K. 1985. Magmas and Magmatic Rocks: An Introduction to Igneous Petrology. Longman, New York.

Okay, A., Tüysüz, O. 1999. Tethyan sutures of northern Turkey. Durand, B., Jolivet, L., Horwarth, E., Seranne, M. (Ed.). The Mediterranean basins: 258 Tertiary extension within the Alpine Orogen. Geological Society of London, Special Publications J560, 475-515.

Öncel, F. 2018. Kuluncak (Malatya) floritlerinin jeokimyasal özellikleri. Yüksek Lisans Tezi, Kahramanmaraş Sütçü İmam Üniversitesi, Fen Bilimleri Enstitüsü, Kahramanmaraş.

Özgenç, İ., Kibici, Y. 1994. The geology and chemical mineralogical properties of the Britholite veins of Başören village (Kuluncak-Malatya), Turkey. Geological Bulletin of Turkey 37, 77-85.

Özgenç, İ., İlbeyli, N. 2009. Geochemical constraints on the petrogenesis of Late Cretaceous alkaline magmatism in east-central Anatolia (Hasancelebi-

Basören, Malatya), Turkey. Mineralogy and Petrology 95,71-85.

Özgül, N. 1971. Toroslar'ın kuzey kesiminin yapısal gelişiminde blok hareketlerinin önemi. Türkiye Jeoloji Kurultayı Bülteni 14(1), 85-101.

Özgül, N. 1984. Stratigraphy and tectonic evolution of the Central Taurides. International Symposium on the Geology of the Taurus Belt, 77-90.

Öztürk, H., Kasapcı, C., Cansu, Z., Hanilci, N. 2016. Geochemical characteristics of iron ore deposits in central-eastern Turkey: an approach to their genesis. International Geology Review 58, 673-1690.

Öztürk, H., Altuncu, S., Hanilçi, N., Kasapçı, C., Goodenough, K. M. 2019. Rare earth element-bearing fuorite deposits of Turkey: an overview, Ore Geology Reviews 105, 426-444.

Parlak, O., Yılmaz, H., Boztuğ, D. 2006. Origin and tectonic significance of the metamorphic sole and isolated dykes of the Divriği ophiolite (Sivas, Turkey): Evidence for slab break-off prior to ophiolite emplacement. Turkish Journal of Earth Sciences 15, 25-45.

Pearce, J. A. 1983. Role of the sub-continental lithosphere in magma genesis at active continental margins. Hawkesworth, C. J., Norry, M. J. (Ed.). Continental Basalts and Mantle Xenoliths, Nantwich, Cheshire. Shiva Publications, 230-249

Pearce, J. A, Haris, N. B. W., Tindle, A. G. 1984. Trace element discrimination diagrams for the tectonic interpretation of granitic rocks. Journal of Petrology 25, 956-983.

Pektaş, A. 2010. Malatya, Kuluncak kuzeyinin ve batısının maden jeolojik incelemesi. Yüksek Lisans Tezi, Ankara Üniversitesi, Fen Bilimleri Enstitüsü, Ankara.

Şen, P., Kuşçu E., Ak, S. 2012. Nadir toprak elementler, özellikleri, cevherleşmeleri ve Türkiye nadir toprak element potansiyeli. MTA Doğal Kaynaklar ve Ekonomi Bülteni 13.

Shand, S. J. 1943. Eruptive Rocks. Their Genesis Composition. Classification, and Their Relation to Ore-Deposits with a Chapter on Meteorite. John Wiley and Sons, New York.

Sun, S., McDonough, W. F. 1989. Chemical and isotopic systematics of oceanic basalt: implications for mantle composition and processes. Saunders, A. D., Norry, M. J. (Ed.). Magmatism in the Ocean Basins. Geological Society of London Special Publication 42, 313-345.

Thirwall, M. F, Smith, T. E., Graham, A. M., Theodorou, N., Hollings, P., Davidson, J. P., Arculus, R. J. 1994. High field strength element anomalies in arc lavas; source or process. Journal Petrology 35, 819-838.

Thompson, R. N., Morrison, M. A., Hendry, G. L., Parry, S. J. 1984. An assessment of the relative roles of crust and mantle in magma genesis: an elemental approach. Philos Translate Society, London, A310 549-590.

Uçurum, A. 1992. Hasançelebi kuzeyinin (KB Malatya) jeolojisi ve volkanitlerin mineralojik - petrografik ve jeokimyasal incelenmesi. Yüksek Lisans Tezi, Cumhuriyet Üniversitesi, Fen Bilimleri Enstitüsü, Sivas, 125.

Uçurum, A., Larson, L. T., Boztuğ, D. 1996. Geology, geochemistry, and petrology of the alkaline subvolcanic trachyte-hosted iron deposit in the Karakuz area, Northwestern Hekimhan–Malatya, Turkey. International Geology Review 38, 995-1005.

Uras, Y., Yalçın, C., Paksoy, M. 2019. Formation and comparison of rare earth element (REE) geochemistry of Malatya fluorite deposits, KSÜ Mühendislik Bilimleri Dergisi 22.

Ünlü, T., Stendal, H. 1989. Divriği bölgesi demir cevheri yataklarının nadir toprak element (NYE) jeokimyası; Orta Anadolu, Türkiye. Türkiye Jeoloji Bülteni 32, 21-37.

Yamık, A., Kibici, Y., Özçelik, İ., Güneş, N. 1995. Kuluncak (Malatya) yöresi fluorit yataklarının genel özellikleri ve zenginleştirilmesi. Endüstriyel Hammaddeler Sempozyumu, İzmir.

Yılmaz, S. 1991. Hekimhan-Hasançelebi (KB Malatya) yöresi jeolojisi ve magmatitlerinin mineralojik-petrografik ve jeokimyasal incelenmesi. Yüksek Lisans Tezi, Cumhuriyet Üniversitesi, Fen Bilimleri Enstitüsü, 256.